Insights into microbial community structure from pairwise interaction networks

by

Logan Massie Higgins

B.A., Lewis & Clark College (2011)

Submitted to the Graduate Program in Microbiology
in partial fulfillment of the requirements for the degree of

Doctor of Philosophy

at the

MASSACHUSETTS INSTITUTE OF TECHNOLOGY

September 2017

Author Signature redacted

Graduate Program in Microbiology
10 August 2017

Certified by Signature redacted

Jeff Gore
Associate Professor, Physics
Thesis Supervisor

Accepted by Signature redacted

Martin F. Polz
Co-Director, Graduate Program in Microbiology

Insights into microbial community structure from pairwise interaction networks

by

Logan Massie Higgins

Submitted to the Graduate Program in Microbiology on 10 August 2017 in partial fulfillment of the requirements for the degree of Doctor of Philosophy in Microbiology

ABSTRACT

Microbial communities are typically incredibly diverse, with many species contributing to the overall function of the community. The structure of these communities is the result of many complex biotic and abiotic factors. In this thesis, my colleagues and I employ a bottom-up approach to investigate the role of interspecies interactions in determining the structure of multispecies communities. First, we investigate the network of pairwise competitive interactions in a model community consisting of 20 strains of naturally co-occurring soil bacteria. The resulting interaction network is strongly hierarchical and lacks significant non-transitive motifs, a result that is robust across multiple environments. Multispecies competitions resulted in extinction of all but the most highly competitive strains, indicating that higher order interactions do not play a major role in structuring this community. Given the lack of non-transitivity and higher order interactions *in vitro*, we conclude that other factors such as temporal or spatial heterogeneity must be at play in determining the ability of these strains to coexist in nature. Next, we propose a simple, qualitative assembly rule that predicts community structure from the outcomes of competitions between small sets of species, and experimentally assess its predictive power using synthetic microbial communities composed of up to eight soil bacterial species. Nearly all competitions resulted in a unique, stable community, whose composition was independent of the initial species fractions. Survival in three-species competitions was predicted by the pairwise outcomes with an accuracy of ~90%. Obtaining a similar level of accuracy in competitions between sets of seven or all eight species required incorporating additional information regarding the outcomes of the three-species competitions. These results demonstrate experimentally the ability of a simple bottom-up approach to predict the structure of communities and illuminate the factors that determine their composition.

Thesis supervisor: Jeff Gore
Title: Associate Professor, Physics

ACKNOWLEDGMENTS

First and foremost, I owe a debt of gratitude towards Jeff for his exemplary mentorship, patience, support, and acceptance. In the same vein, I cannot overstate my appreciation for Jonathan. He is the ultimate role model, both in the lab and out in the real world.

I am also grateful to the other members of the Gore Lab and the Physics of Living Systems community for their good humor, camaraderie, and succor, and for introducing me to so many of my other friends over the years. I will sorely miss their daily companionship going forward, but fully anticipate continuing these friendships beyond the confines of Tech Square.

Ty, Kerry, and Monica each deserve special recognition for their heroic feats of organization and their unfailingly sunny personalities, even in the face of my many administrative inadequacies.

To my classmates in the Micro program and its directors, past and present: Alan, Kris, Mike, and Martin, I give my thanks for their dedication to this wonderful community. I would also like to particularly acknowledge Bonnielee, who has been the nexus of the program since its inception. I wish her all the best in her retirement.

I'm thankful to my committee members, Martin and Otto, for their expertise and agreeability, and to my outside committee member, Benjamin Wolfe, for gamely showing up to my defense.

Over the years, I've been lucky to be supported by an excellent team of care providers at MIT Medical. A special thanks to Drs. Shapiro, Kantrowitz, Ayala, and Fernandes; and to Evan, Kate, Maya, and the group. I don't know where I would be without them.

A huge thanks to Tommaso, whose companionship has been very meaningful to me. Finally, I'm grateful for the unwavering support of my family: Stewart, Jennifer, and Hannah. I know that they have always thought the world of me, no matter what.

Thank you all.

TABLE OF CONTENTS

LIST OF FIGURES

Chapter Two

Chapter Three

LIST OF TABLES

Chapter Two

Chapter Three

CHAPTER ONE

Introduction

1.1. Historical and modern perspectives on the origins and maintenance of diversity

The Yale limnologist G. Evelyn Hutchinson (1903-1991) had a profound influence on the field of ecology in the 20th century, and on the our understanding of the maintenance of diversity in particular. Hutchinson is perhaps best known for his so-called "paradox of the plankton[1]." With this example, he calls attention to the tension between the intuitively undisputable competitive exclusion principle[2] and the equally undisputable observation that multiple competing species are regularly found coexisting in nature – his favored example being the seemingly paradoxical coexistence of many highly similar species of plankton in a relatively homogeneous aquatic environment. The basic tenets of the competitive exclusion principle are as old as the field of ecology itself, being reflected in Charles Darwin's construction of the theory of natural selection[3] and Georgy Gause's mathematical formalization of the struggle for existence[4].

Of course, real ecosystems are incalculably more complex than the simple models we develop to describe them; in his paper, Hutchinson provides a laundry list of complicating factors that could contribute to the coexistence of his plankton species, ranging from microscale environmental variations allowing for niche separation, to the stabilizing effects of commensalism and predation, to the existence of non-equilibrium conditions with constant species turnover and replenishment of species from external sources[1]. These ideas were have continued to form the basis of much of theoretical[5] and empirical[6] community ecology. In contrast, the idea that neutral processes could have strong implications for the structure of ecological communities represents a distinct, yet complementary school of thought[7,8].

While much of ecological theory has been developed with an eye towards macro-organisms, microbial communities are equally as deserving of attention, and have a number of notable differences from their larger scale counterparts. Microorganisms experience and move through spaces in ways that counteract our intuition; they reproduce and evolve on short timescales,

leading to complex eco-evolutionary dynamics; and they interact with each other in subtle and varied ways. In recent years, the rise of metagenomics has revolutionized the field of microbial ecology, allowing researchers to investigate microbial community structure in a way that is impossible with traditional culture-based methods[9,10]. Nevertheless, there is still a role for experimental approaches in microbial community ecology, particularly in order to investigate the factors that determine community structure and to validate techniques for engineering microbial consortia.

1.2. Methods and motivations for investigating ecological communities

A greater understanding of how microbial communities are assembled could be useful for a variety of human endeavors. For example, synthetic biologists may be interested in ways to construct ecological communities that maximize the production or degradation of a particular chemical compound, while in clinical settings, synthetic human-associated microbial communities could be used to help treat or prevent diseases[11] .At the same time, conservationists are concerned with preserving existing communities in the face of stark biotic and abiotic challenges. Since microbes play an outsized role in how ecosystems function throughout the biosphere[12], it is essential to understand both the patterns and processes of microbial community assembly in order to effectively respond to global change. Finally, insights from microbial ecology can be translated to macro-scale ecological communities and processes, with largely overlapping applications. In addition to the intrinsic importance of microbes, model microbial systems can be ideal go-betweens for the application of ecological theory to nature[13,14]. Experiments can be performed in minute volumes over short timescales of a few days or weeks, rather than months, years, or even decades, as is often the case with macro-scale ecology[15,16,17].

1.3. Aims of this thesis

When I formally submitted my thesis proposal in the spring of 2015, I did so with two specific aims:

1. To conduct pairwise competition experiments using bacterial strains isolated from natural soil communities to investigate the relative importance of resource competition versus chemically mediated antagonism in bacterial competition.

2. To conduct pairwise competition experiments using a synthetic bacterial community in order to investigate the possibility of using observations of competitive exclusion, coexistence, and/or bistability between pairs of species in order to qualitatively predict the outcome of competition among three or more species.

I present here the results of these efforts. As I have learned to expect, things did not go entirely as expected. In Chapter Two, my colleagues and I describe the process of establishing a model system of naturally co-occurring soil bacteria and measuring competitive outcomes between them in order to address my first aim. When we conceived of this experiment, we did so hoping to investigate the links among phylogenetic relatedness, the strength of competition, resource overlap, and the prevalence of antibiotic mediated antagonism in bacteria. The model system proved to be ill-suited for this aim because it is characterized by intense competition resulting in a strongly hierarchical interaction network with echoes of Hutchinson's paradox. In Chapter Three, we propose a simple bottom-up approach for predicting the structure of a multispecies community and test it in a model bacterial system. We found that our approach predicts community structure with reasonable accuracy based on simple, qualitative measurements of the type performed in Chapter Two.

1.4. References

---

[1] Hutchinson, G. E. The paradox of the plankton. *Am. Nat.* **95,** 137-145 (1961).

[2] Hardin, G. The competitive exclusion principle. *Science* **131,** 1292-1297 (1960).

[3] Darwin, C. *On the Origin of Species by Means of Natural Selection* (1859).

[4] Gause, G. F. Experimental studies on the struggle for existence. *J. Exper. Biol.* **9,** 389-402 (1932).

[5] Chesson, P. Mechanisms of the maintenance of species diversity. *Annu. Rev. Ecol. Syst.* **31,** 343-366 (2000).

[6] Silvertown, J. Plant coexistence and the niche. *Trends Ecol. Evol.* **19,** 605-611 (2004).

[7] Adler, P. B., HilleRisLambers, J. & Levine, J. M. A niche for neutrality. *Ecol. Lett.* **10,** 95-104 (2006).

[8] Chave, J. Neutral theory and community ecology. *Ecol. Lett.* **7,** 241-253 (2004).

[9] Caporaso, J. G., Lauber, C. L., Walters, W. A., Berg-Lyons, D., Lozupone, C. A., Turnbaugh, P. J., Fierer, N., & Knight, R. Global patterns of 16S rRNA diversity at a depth of millions of sequences per sample. *Proc. Natl. Acad. Sci. USA* **108,** 4516-4522 (2011).

[10] The Human Microbiome Project Consortium. Structure, function, and diversity of the healthy numan microbiome. *Nature* **486,** 207-214 (2012).

[11] Brenner, K., You, L. & Arnold, F. H. Engineering microbial consortia: a new frontier in synthetic biology. *Trends Biotech.* **26,** 483-489 (2008).

[12] Newman, D. K. & Banfield, J. F. Geomicrobiology: how molecular-scale interactions underpin biogeochemical systems. *Science* **296,** 1071-1077 (2002).

[13] Jessup, C. M., Kassen, R., Forde, S. E., Kerr, B., Buckling, A., Rainey, P. B. & Bohannan, B. J. M. Big questions, small worlds: microbial model systems in ecology. *Trends Ecol. Evol.* **19,** 189-197 (2004).

[14] Friedman, J. & Gore, J. Ecological systems biology: the dynamics of interacting populations. *Curr. Opin. Syst. Biol.* **1,** 114-121 (2017).

[15] Elton, C. & Nicholson, M. The ten-year cycle in numbers of the lynx in Canada. *J. Anim. Ecol.* **11,** 215-244 (1942).

[16] Connell, J. H. Effects of competition, predation by *Thais lapillus*, and other factors on natural populations of the barnacle *Balanus balanoides*. *Ecol. Monogr.* **31,** 61-104 (1961).

[17] Tilman, D. & Downing, J. A. Biodiversity and stability in grasslands. *Nature* **367,** 363-365 (1994).

CHAPTER TWO

Naturally co-occurring soil bacteria exhibit a robust competitive hierarchy and lack of non-transitive interactions

by Logan Higgins, Jonathan Friedman, Hao Shen, and Jeff Gore

2.1. Overview

Despite their small size, microbes play outsized roles at multiple ecosystem scales, from the planetary[18] to that of the human individual[19]. Like their macroscopic counterparts, microbes typically exist in diverse communities whose functions are intimately related to their structure. Diversity impacts an ecological community's stability, resilience to perturbations, and its ability to provide ecosystem services[20]. Therefore, a long-standing area of interest in microbial ecology has been understanding the factors that give rise to the diversity observed within microbial communities[21,22]. A better understanding of the structure of microbial communities is desirable for both managing existing microbial communities[23] and, eventually, engineering them *de novo*[24].

One approach to studying the structure of a community is to investigate the network of underlying interactions among its constituent members[25]. These interactions can be classified according to the effect the interaction has on the fitness of the interacting species. Since interspecific competition is thought to be a dominant factor in determining whether a given species can persist in a community[26,27], the network of competitive interactions between species may be informative of the structure of the community within which the interaction takes place. Features of competitive interaction networks that could contribute to community diversity can include non-transitive motifs such as the classic rock-paper-scissors triad[28], network modularity[29], or overall trends towards weak interactions among species[30].

While non-transitivity in particular is often cited as a potential driver of interspecies coexistence[31,32,33], the degree to which it occurs in natural communities remains largely unknown. Indeed, Levine and colleagues recently asserted that despite the theoretical potential of non-transitive interactions to stabilize community structure, there is scant evidence that they are

widespread in natural systems, and that further empirical studies are warranted[34]. Recent experimental work using a field-parameterized model of competition in annual plants[35] and naturally co-occurring *Streptomyces* bacteria[36] suggest that rock-paper-scissors type interactions may be less common in natural communities than we might assume; however, further studies of competitive interaction networks in diverse ecological communities are warranted, particularly among phylogenetically diverse natural assemblages.

Here, we add to this small but growing body of research that suggests that non-transitive interactions may play a less significant role in maintaining species diversity than is commonly assumed. We use a model system composed of soil-dwelling heterotrophic bacteria competing in all pairwise combinations in laboratory culture and find that the overarching feature of the resulting interaction network is a strong competitive hierarchy, a feature that is naturally at odds with a high incidence of non-transitivity. Therefore, in the natural environment of these bacteria, other factors must be at play that account for their ability to co-occur.

2.2. Results

To probe the network of pairwise interactions in a community of diverse microbes, we isolated a collection 20 strains of naturally co-occurring heterotrophic soil bacteria drawn from 16 species across seven genera and five families (Fig. 2.1a and Methods). The strains were isolated from a single grain of soil. Similar to ref[37], we co-inoculated all pairwise combinations of the strains at varying initial fractions and propagated them through at least five growth-dilution cycles. During each growth cycle, cells were cultured for 24 hours and then diluted by a factor of 100 into fresh media. The final outcome of competition was determined by plating the cultures on solid agar and counting colonies, which are morphologically distinct (Fig. 2.1c and Supplementary Fig. 2.1).

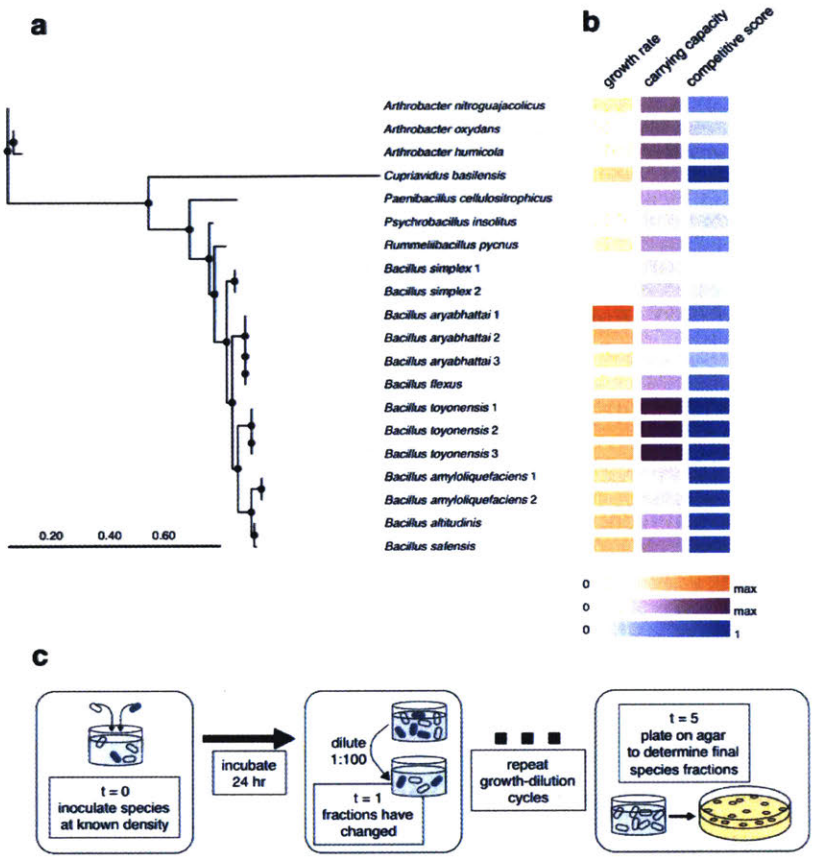

Figure 2.1. Twenty strains of bacteria isolated from a single grain of soil were competed against each other in all pairwise combinations. a, Phylogenetic tree of the 20 strains used in this study. Tree was constructed using the full 16S gene. **b**, Growth rate (orange) and carrying capacity (purple) of each strain in monoculture, as well as competitive score against other strains (blue). Lighter shades correspond to lower values, while darker shades correspond to higher values. **c**, We competed all 190 pairwise combinations of the soil isolates in the laboratory. Colonies of different strains are visually distinct, allowing determination of final species fractions at the end of competition.

Pairwise competitions resulted in one of three qualitatively different outcomes: exclusion, coexistence, or bistability (Fig. 2.2a-c and Methods). In 153 of the 190 pairs (81%), only one strain could invade the other and drove it to extinction, an outcome we call exclusion. Nineteen pairs (10%) were mutually invasible, and thus exhibited coexistence over the time span of the experiment. Finally, 15 pairs (8%) were mutually non-invasible, an outcome that we call bistability. In a small number of pairs (3; 2%), we were unable to determine the outcome due to

contamination. Due to the high incidence of exclusion outcomes, we conclude that these strains interact in the experimental environment primarily through competition.

As a measure of the overall competitive ability of a given strain, we calculated its average competitive score, which is simply the strain's mean final fraction in competition across all partners. The competitive scores that we measured spanned nearly the entire possible range, from a low of 0.03 to a high of 0.91 (Fig. 2.1b and Supplementary Table 2.1).

The strains exhibit a strong competitive hierarchy. Very few strains were able to exclude a strain with a higher competitive score; out of 187 pairwise competitions measured, only five resulted in the lower-ranked strain excluding the higher-ranked one (Fig. 2.2d). The degree of hierarchy in this interaction network is highly significant when compared to networks with randomized outcomes ($p < 10^{-19}$; Fig. 2.2e). To assess whether the hierarchical pattern was specific to a particular environment, we repeated the competitions with subsets of the 20 primary strains in different growth media and with different dilution rates (Supplementary Fig. 2.2). Not only were the resultant interaction networks of these experiments also highly hierarchical (Fig. 2.2f), but there were also correlations between the strains' competitive scores across the different experimental conditions (Supplementary Fig. 2.3). Thus, we conclude that hierarchy in pairwise competition is a central feature of this model community.

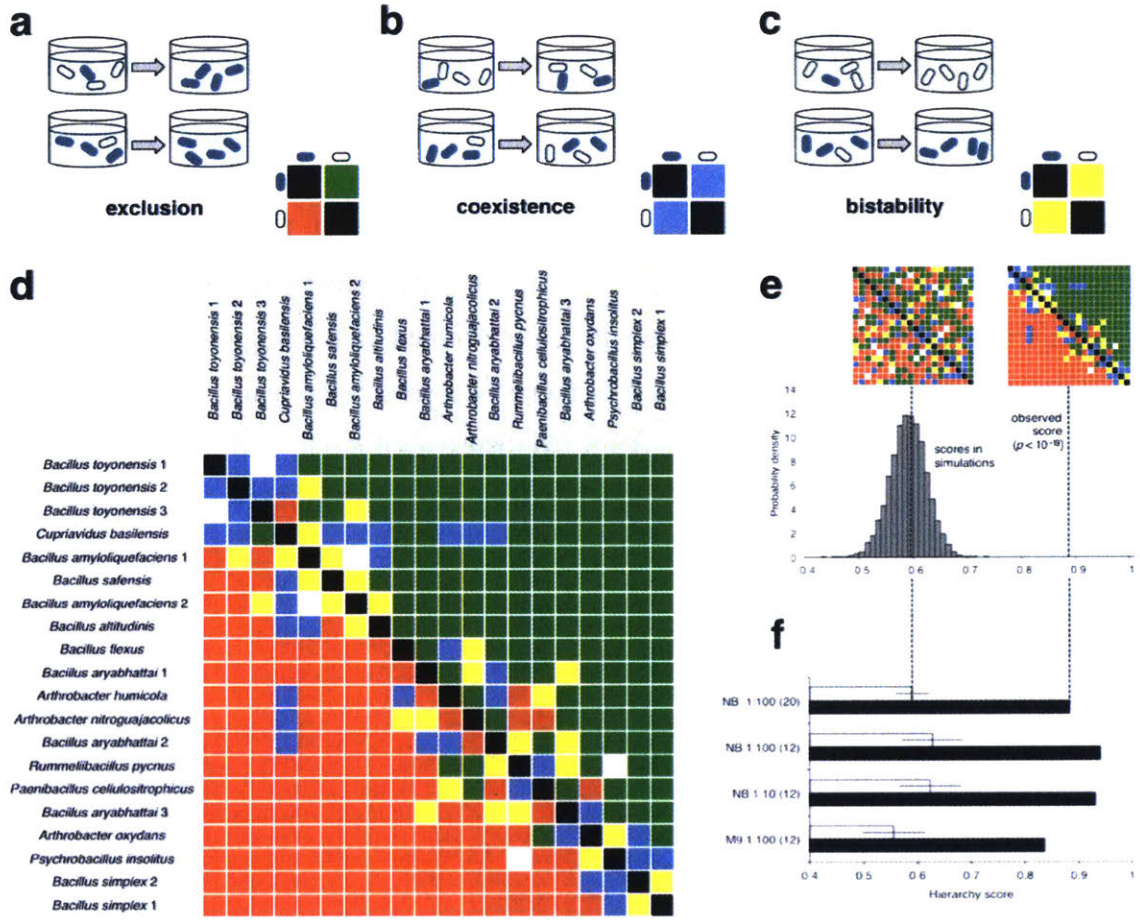

Figure 2.2. The network of pairwise interactions among strains is strongly hierarchical. a-c, Changes in relative abundance over time in three hypothetical pairs: one in which the outcome was competitive exclusion; one in which the outcome was stable coexistence; and one in which the outcome was bistability. The color-coded matrices inset into each diagram indicate the qualitative outcome for the row species in competition with the column species. **d**, Pairwise outcome matrix for the entire 20-strain assemblage. Outcomes are color coded as for **a-c**, with white indicating an indeterminate outcome. Rows and columns are sorted in decreasing order of each strain's competitive score. **e**, Histogram of so-called "hierarchy scores" for randomized outcome matrices. The hierarchy score for a given matrix is calculated by summing the final fractions of the row strain in competition with the column strain across all row-column pairs in the upper triangle. The difference is highly significant ($p < 10^{-20}$). **f**, Hierarchy scores for pairwise interaction networks associated with varying environmental conditions and the corresponding randomized networks. NB: 0.2X nutrient broth. M9: 1X M9 minimal medium supplemented with 0.2% casamino acids, 0.4% glycerol, and 1 mM thiamine HCl. Dilution rates were either 1:100 or 1:10 per 24 hr, and experiments consisted of either the full complement of 20 bacterial strains or subsets of 12, as indicated in parentheses. Error bars represent +/– 1 s.d.

Next, we asked what characteristics of a strain might best predict its performance in competition. We hypothesized that strains that grow robustly in monoculture might have competitive advantages over strains that grow more poorly, as indicated by large differences in early growth rates and/or carrying capacities between the strains. Indeed, we found that growth rate was positively correlated with competitive score (Fig. 2.3a) and that the faster-growing strain excluded the slower one 67% of the time (Fig. 2.3c). Carrying capacity in monoculture was less predictive of competitive superiority, but still outperformed random guessing (Fig. 3b and Supplementary Fig. 2.4). While differences in these two parameters can be indicators of the likelihood of a given competitive outcome, there are many exceptions, and, indeed, some of the stronger competitors do not necessarily have correspondingly strong single-species growth parameters.

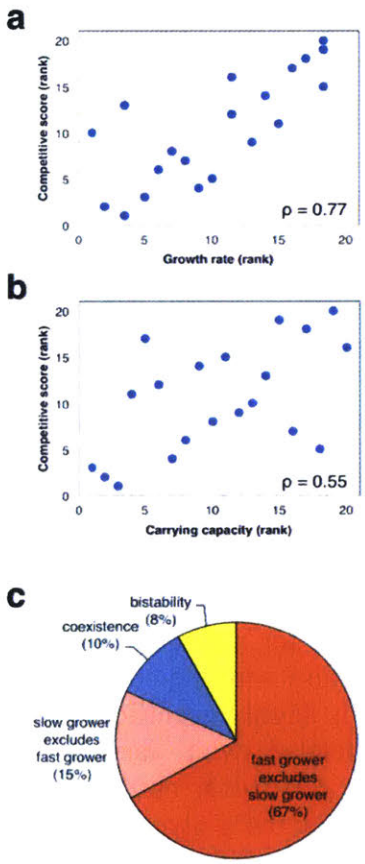

Figure 2.3. Differences in growth parameters frequently predict the outcome of competition. a, **b**, Correlation between rank in growth rate (as estimated using a time-to-threshold method) or rank in carrying capacity (as measured using OD_{600}) and rank in

competitive score. **c**, Distribution of competitive outcomes for all pairs, with pairs that exhibit exclusion differentiated according to whether the faster or slower grower excludes the other.

An important corollary of the high degree of hierarchy we observed in the interaction network is that non-transitive motifs are vanishingly rare. Non-transitive motifs are instances in which a clear competitive hierarchy among members of a sub-group does not exist, the classic example being a rock-paper-scissors (RPS) triad (Fig. 2.4a). Of the 987 triads in our collection for which complete pairwise outcome data are available, only three (0.3%) display the RPS topology. This number is significantly less than is found in randomized networks, where on average 14% of triads were RPS ($p < 10^{15}$; Fig. 2.4b). Furthermore, the three triads that we classify as RPS each feature strains that display unusually high variability from experiment to experiment, possibly due to rapid evolution, and further efforts to characterize these triads failed to reproduce the non-transitive network topology. As dictated by its hierarchical structure, our network is also highly enriched for perfectly hierarchical feedforward loops (Fig. 2.4a), which were observed in over 50% of triads (Fig. 2.4b). Due to the paucity and irreproducibility of observable non-transitive relationships among our strains *in vitro*, we conclude that such relationships are unlikely to be a significant contributor to their coexistence in a natural environment.

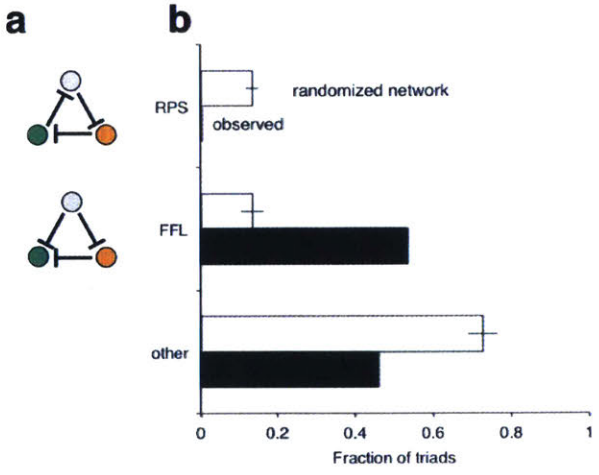

Figure 2.4. The interaction network contains very few cycles. a, Schematics of a perfectly non-transitive motif (i.e., rock-paper-scissors; top) and a perfectly transitive motif (i.e., feedforward loop; bottom) **b**, There were significantly fewer rock-paper-scissors triads and

significantly more feedforward loops in the network of observed outcomes as compared to 1000 randomized networks. Error bars represent +/– 1 s.d.

Given the hierarchical structure of the pairwise interaction network, we wondered about the potential of higher-order interactions and indirect effects among our strains to give rise to a diverse community. To address this, we inoculated three replicate cultures with equal proportions of all strains and propagated them through five growth-dilution cycles (Fig. 2.5b). The resulting assemblages were highly replicable, and consisted of three strains representing some of the strongest competitors in pairwise experiments (Fig. 2.5a,c), all of which were found to coexist with each other in pairwise competition. Notably, this combination of survivors was consistent with the simple community assembly rule put forth in ref[37]: namely, that a strain is expected to survive in multispecies competition if and only if it is not excluded by any other surviving species. Since pairwise outcomes alone are sufficient to predict the outcome of multispecies competition in this environment, we conclude that higher-order interactions are unlikely to play a major role in structuring this community.

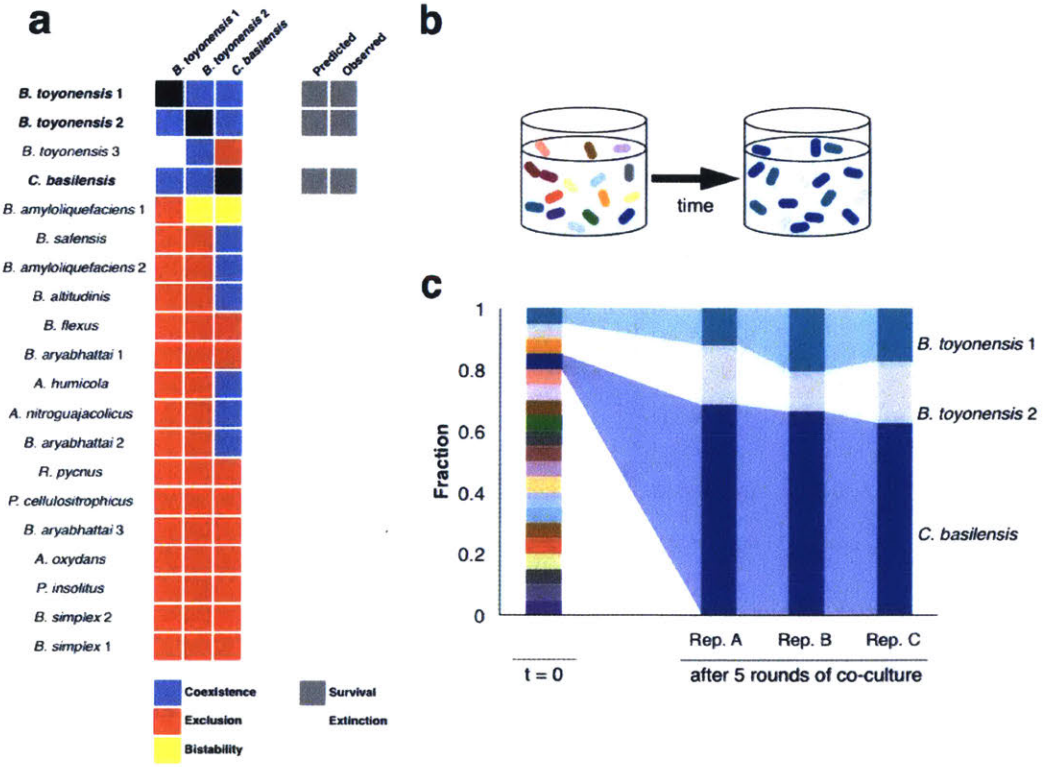

Figure 2.5. As predicted by pairwise outcomes, only three species survive in all-versus-all competition. **a**, Predictions of the outcome of multispecies competition based on pairwise outcomes. **b**, All strains were mixed in equal proportion and allowed to reach equilibrium. **c**, In three replicate cultures, only the same three strains survived, each of which was found to coexist with the others in pairwise experiments.

2.3. Discussion

Theory predicts that there are may factors that can contribute to the generation and maintenance of diversity in ecological communities. Non-transitivity, cooperation, bistability, weak interactions, multiple limiting factors, and spatial or temporal segregation have all been hypothesized to play a role[38]; however, there is little empirical data regarding the relative importance of each of these factors in actual communities. Here, we explored one such community. Our results led us to de-emphasize some factors (e.g., frequent bistability, non-transitivity, and higher order interactions) while drawing increased focus on others (e.g., multiple limiting factors and spatial or temporal segregation). Despite these hints, we still do not completely understand the processes that give rise to the diversity we observe in nature.

Given that soil is a heterogeneous mixture with a multitude of microhabitats, microbial co-occurrence in soil may be facilitated by niche separation and spatial demixing. This would allow the coexistence of strains with strong inhibitory interactions in well-mixed environments. Microbes in soil also experience a strongly fluctuating environment, which can lead to coexistence of multiple strains over time via the soil spore bank. Members of the genus *Bacillus* are particularly well known for their spore-forming ability, which may allow them to persist in a non-vegetative, and therefore non-competitive state, until conditions favor their growth[39]. Finally, given the strong selection for strains that thrive under laboratory conditions, it is plausible that the strains used in these experiments are in fact only minor players in the context of the larger bacterial community in their native habitat, and isolated competition experiments in the lab do not reflect the full complexity of interactions affecting these microbes in nature.

Simulations of our experimental system using the generalized Lotka-Volterra model (gLV) predicted that, if the underlying ecological interactions among species are assigned at random, the pairwise interaction network should become less hierarchical with decreasing death rates

(Supplementary Fig. 2.5). In order to test this hypothesis, we competed a subset of pairs while experimentally reducing the daily dilution rate from 1:100 to 1:10 (Fig. 2.2f). The hierarchical network structure was robust to this manipulation (Supplementary Fig. 2.2a,b), and remained highly correlated with growth rates in monoculture. While it is possible that reducing the death rate further could weaken the hierarchy, we can nevertheless not rule out the possibility of an underlying competitive hierarchy that is correlated with but distinct from the strains' growth rates.

This experimental system also gives us the opportunity to test the importance of higher order interactions in shaping communities. Higher order interactions are said to take place when the presence of an additional species changes the interaction between two existing species[40], and have the potential to contribute to the maintenance of species diversity[41]. In bacterial systems, this can be driven by complex networks of selective antibiotic production and sensitivity[42]. Despite the potential for higher order interactions in our model community, our simple assembly rule[37], which disregards higher order interactions entirely, accurately predicted the survivors in all-versus-all competition *in vitro*, suggesting that higher order interactions are not a major driver of community structure in this instance.

The observation of high levels of diversity in communities of competing organisms is a long-standing paradox in community ecology[43]. In this work, we showed that a bottom-up approach to studying community assembly can be useful in narrowing down the range of possible explanations for the diversity we observe in nature. However, this approach necessitates removing the organisms from their natural environment, including the larger community in which the species of interest are embedded. Future work combining *in vitro* competition experiments with a more mechanistic understanding of the influence of environment on species survival would help to further explain the persistence of diversity in nature.

2.4. Methods

Strain isolation and identification. Bacterial strains were isolated from a single grain of soil collected in September, 2015 in Cambridge, Mass., U.S.A. The grain weighted ~1 mg and was

handled using sterile technique. The grain was washed in phosphate-buffered saline (PBS) and serial dilutions of the supernatant were plated on nutrient agar (0.3% yeast extract, 0.5% peptone, 1.5% bacto agar) and incubated for 48 hr at room temperature. Isolated colonies were sampled and cultured at room temperature in 5 mL nutrient broth (0.3% yeast extract, 0.5% peptone) for 48 hr. To ensure purity, the liquid cultures of the isolates were diluted in PBS and plated on nutrient agar. Single colonies picked from these plates were once again grown in in nutrient broth for 48 hr at room temperature and the resulting stocks were stored in 20% glycerol at -80° C.

The 16S rRNA gene was sequenced via Sanger sequencing of DNA extracted from glycerol stocks carried out at GENEWIZ (South Plainfield, New Jersey, U.S.A.). Sequencing was performed in both directions using the company's proprietary universal 16S rRNA primers, yielding assembled sequences ~1100 nt in usable length. Species names were assigned using the Ribosomal Database Project's Seqmatch module[44] based on the type strain with the highest seqmatch score relative to the query strain. Three strains (*B. toyonensis* 1, 2, and 3) had identical 16S rRNA sequences, and were therefore differentiated using a 404-bp fragment of the *pyrE* gene amplified using the primers 5′-TCGCATCGCATTTATTAGAA-3′ and 5′-CCTGCTTCAAGCTCGTATG-3′ following protocols described in ref[45]. A list of the strains used, their competitive scores, and inferred growth parameters is given in Supplementary Table 2.1. For phylogenetic analysis, sequences were aligned using MUSCLE[46] and a tree was constructed using PhyML 3.0[47,48].

Estimation of single-species growth parameters. The carrying capacity of each individual strain was estimated to be its optical density at 600 nm (OD_{600}) in 0.2X nutrient broth after five repeated growth-dilution cycles, starting from an initial OD_{600} of 3×10^{-3}. Growth curves at OD_{600} were measured in flat-bottomed 96-well microtiter plates (BD Biosciences) with lids sealed with Parafilm in a Tecan Infinite M200 Pro plate reader over 48 hr at 25° C with maximum shaking. An approximation of the exponential growth rate of each individual strain was extracted from the growth curves using the time each strain took to reach a threshold optical density. The time-to-threshold method was chosen over other estimates of growth rate due to wide variations in growth patterns across the strains, which led to difficulties in fitting parameters to other population growth models.

Competition experiments. Prior to competition experiments, cells were streaked out on nutrient agar plates, grown for 48 hr at room temperature, and then stored at 4° C for up to two weeks. Single colonies were picked from these plates and grown for 24 hr at room temperature in 0.2X nutrient broth.

The competitions were initiated by diluting each individual strain in 0.2X nutrient broth to an OD_{600} of 3×10^{-3}. The diluted cultures were then mixed by volume to the desired starting ratios of 0.05/0.95 and 0.95/0.05 (Strain A/Strain B). The competitions were performed in 200 mL volumes in flat-bottomed 96-well microtiter plates sealed with Titer Tops® polyethylene sealing films (Diversified Biotech). For each growth-dilution cycle, the cultures were incubated at 25° C and shaken at 900 rpm for 24 hr. At the end of each cycle, the cultures were thoroughly mixed and then diluted by a factor of 100 into fresh media. OD_{600} was measured at the end of each cycle, and final species fractions were estimated after five (or, in the case of initially low plating density, seven) cycles.

To measure the final species fractions, the co-cultures were diluted by a factor of 10^4-10^6 (depending on OD_{600}) in PBS. Seventy-five mL of the diluent was plated onto 10 cm Petri dishes containing 25 mL of nutrient agar and incubated at room temperature for 48 hr. All but a small fraction of the strain pairs have distinct colony morphologies, so species fractions were estimated by counting colonies of each type (median: 51 colonies per plate). Next-generation sequencing of a subset of the co-cultures affirmed the accuracy of the plating technique (Supplementary Fig. 2.6).

Determining the outcome of competition. The result of competition was classified as one of three outcomes: exclusion of a single strain, coexistence of both strains, or bistability. A strain was said to exclude its competitor if it was the sole strain observed from both starting frequencies after 5 cycles, or if it excluded its competitor when starting from an initial frequency of 0.95 and achieved a frequency of 0.85 or greater when starting from an initial frequency of 0.05. Pairs were considered bistable if the strain that started out at a frequency of 0.95 excluded the competitor. All other outcomes were classified as coexistence.

Calculating competitive score and network hierarchy score. The competitive score s_i of each strain i was defined as its mean fraction $fr_{i,j}$ after co-culture with each of the $n - 1$ competitor strains:

$$s_i = \left(\sum_{i \neq j} fr_{i,j}\right) \Big/ (n-1)$$

The hierarchy score (*h.s.*) for an n-member network is calculated as:

$$\text{h.s.} = \sum_{s_i > s_j} fr_{i,j}$$

The network hierarchy score for the observed set of competitive outcomes was then compared against the distribution of scores for 10,000 simulated networks in which each pair was randomly assigned an outcome of exclusion, coexistence, or bistability with probability proportional to the incidence of each outcome in the empirical dataset. The resulting distribution of hierarchy scores was approximated using the normal distribution to determine p-values.

Identifying network motifs. The frequencies of distinct topologies among the $\binom{20}{3} = 1140$ three-strain networks were enumerated using the FANMOD software package[49]. Random networks were simulated by assigning the outcome of exclusion to each pair of strains within the simulated network with the probability 0.818, which is equal to the fraction of pairs in the empirical dataset with that relationship. The occurrence of rock-paper-scissors and feedforward loop motifs were enumerated for 1000 simulated networks and approximated by a normal distribution to determine p-values.

[18] Falkowski, P., Fenchel, T., & Delong, E. The microbial engines that drive Earth's biogeochemical cycles. *Science* **320,** 1034-1039 (2008).

[19] Flint, H. J., Scott, K. P., Louis, P. & Duncan, S. H. The role of the gut microbiota in nutrition and health. *Nat. Rev. Gastroenterol. Hepatol.* **9,** 577-589 (2012).

[20] Hooper, D. U., Chapin, F. S., Ewel, J. J., Hector, A., Inchausti, P., Lavorel, S., Lawton, J. H., Lodge, D. M., Loreau, M., Naeem, S., Schmid, B., Setala, H., Symstad, A. J., Vandermeer, J. & Wardle, D. A. Effects of biodiversity on ecosystem functioning: a consensus of current knowledge. *Ecol. Monogr.* **75,** 3-35 (2005).

[21] Torsvik, V., Ovreas, L. & Thingstad, T. F. Prokaryotic diversity – magnitude, dynamics, and controlling factors. *Science* **296,** 1064-1066 (2002).

[22] Fierer, N. & Jackson, R. B. The diversity and biogeography of soil bacterial communities. *Proc. Natl. Acad. Sci. USA* **103,** 626-631 (2006).

[23] Antunes, L. C. M., Han, J., Ferreira, R. B. R., Lolic, P., Borchers, C. H. & Finlay, B. B. Effect of antibiotic treatment on the intestinal metabolome. *Antimicrob. Agents Ch.* **55,** 1494-1503 (2011).

[24] Lindemann, S. R., Bernstein, H. C., Song, H. S., Fredrickson, J. K., Fields, M. W., Shou, W. Y., Johnson, D. R. & Beliaev, A. S. Engineering microbial consortia for controllable outputs. *ISME J.* **10,** 2077-2084 (2016).

[25] Proulx, S. R., Promislow, D. E. L. & Phillips, P. C. Network thinking in ecology and evolution. *Trends Ecol. Evol.* **20,** 345-353 (2005).

[26] Gurevitch, J., Morrow, L. L., Wallace, A. & Walsh, J. S. A metaanalysis of competition in field experiments. *Am. Nat.* **140,** 539-572 (1992).

[27] Foster, K. R. & Bell, T. Competition, not cooperation, dominates interactions among culturable microbial species. *Curr. Biol.* **22,** 1845-1850 (2012).

[28] Kerr, B., Riley, M. A., Feldman, M. W. & Bohannan, B. J. M. Local dispersal promotes biodiversity in a real-life game of rock-paper-scissors. *Nature* **418,** 171-174 (2002).

[29] Mayfield, M. M. & Levine, J. M. Opposing effects of competitive exclusion on the phylogenetic structure of communities. *Ecol. Lett.* **13,** 1085-1093 (2010).

[30] Coyte, K. Z., Schluter, J. & Foster, K. R. The ecology of the microbiome: networks, competition, and stability. *Science* **350,** 663-666 (2015).

[31] Laird, R. A. & Schamp, B. S. Competitive intransitivity promotes species coexistence. *Am. Nat.* **168,** 182-193 (2006).

[32] Reichenbach, T., Mobilia, M. & Frey, E. Mobility promotes and jeopardizes biodiversity in rock-paper-scissors games. *Nature* **448,** 1046-1049 (2007).

[33] Allesina, S. & Levine, J. M. A competitive network theory of species biodiversity. *Proc. Natl. Acad. Sci. USA* **108,** 5638-5642 (2011).

[34] Levine, J. M., Bascompte, J., Adler, P. B. & Allesina, S. Beyond pairwise mechanisms of species coexistence in complex communities. *Nature* **546,** 56-64 (2017).

[35] Godoy, O., Stouffer, D. B., Kraft, N. J. B. & Levine, J. M. Intransitivity is infrequent and fails to promote annual plant coexistence without pairwise niche differences. *Ecology* **98,** 1193-1200 (2017).

[36] Wright, E. S. & Vetsigian, K. H. Inhibitory interactions promote frequent bistability among competing bacteria. *Nat. Commun.* **7,** 11274 (2016).

[37] Friedman, J., Higgins, L. M. & Gore, J. Community structure follows simple assembly rules in microbial microcosms. *Nat. Ecol. Evol.* **1,** 0109 (2017).

[38] HilleRisLambers, J., Adler, P. B., Harpole, W. S., Levine, J. M. & Mayfield, M. M. Rethinking community assembly through the lens of coexistence theory. *Annu. Rev. Ecol. Evol. S.* **43,** 227-248 (2012).

[39] Smit, E., Leeflang, P., Gommans, S., van den Broek, J., van Mil, S. & Wernars, K. Diversity and seasonal fluctuations of the dominant members of the bacterial soil community in a wheat field as determined by cultivation and molecular methods. *Appl. Environ. Microbiol.* **67,** 2284-2291 (2001).

[40] Billick, I. & Case, T. J. Higher order interactions in ecological communities: what are they and how can they be detected? *Ecology* **75,** 1529-1543 (1994).

[41] Bairey, E., Kelsic, E. D. & Kishony, R. High-order interactions shape ecosystem diversity. *Nat. Commun.* **7,** 12285 (2016).

[42] Czárán, T. L., Hoekstra, R. F. & Pagie, L. Chemical warfare between microbes promotes biodiversity. *Proc. Natl. Acad. Sci. USA* **99,** 786-790 (2002).

[43] Hutchinson, G. E. The paradox of the plankton. *Am. Nat.* **95,** 137-145 (1961).

[44] Cole, J. R., Wang, Q., Fish, J. A., Chai, B., McGarrell, D. M., Sun, Y., Brown, C. T., Porras-Alfaro, A., Kuske, C. R. & Tiedje, J. M. Ribosomal Database Project: data and tools for high throughput rRNA analysis. *Nucleic Acid Res.* **42,** D633-D642 (2014).

[45] Helgason, E., Tourasse, N. J., Meisal, R., Caugant, D. A. & Kolstø, A.-B. Multilocus sequence typing scheme for bacteria of the *Bacillus cereus* group. *Appl. Environ. Microbiol.* **70,** 191-201 (2004).

[46] Edgar, R. C. MUSCLE: multiple sequence alignment with high accuracy and high throughput. *Nucleic Acids Res.* **19,** 1792-1797 (2004).

[47] Guindon, S., Dufayard J. F., Lefort, V., Anisimova, M., Hordijk, W. & Gascuel, O. PhyML 3.0: new algorithms, methods and utilities. *Syst. Biol.* **59,** 307-321 (2010).

[48] Lefort, V., Longueville, J.-E. & Gascuel, O. SMS: Smart Model Selection in PhyML. *Mol. Biol. Evol.* msx149 (2017).

[49] Wernicke, S. & Rasche, F. FANMOD: a tool for fast network motif detection. *Bioinformatics* **22,** 1152-1153 (2006).

2.6. Supplementary Materials

Bacillus aryabhattai 1 | *Bacillus toyonensis* 1 | *Bacillus amyloliquefaciens* 1 | *Cupriavidus basilensis* | *Bacillus altitudinis*

Supplementary Figure 2.1. Colony morphology of selected strains. Each strain possesses a distinct morphotype when plated on nutrient agar, allowing for estimation of the relative abundance of each strain following co-culture in liquid media.

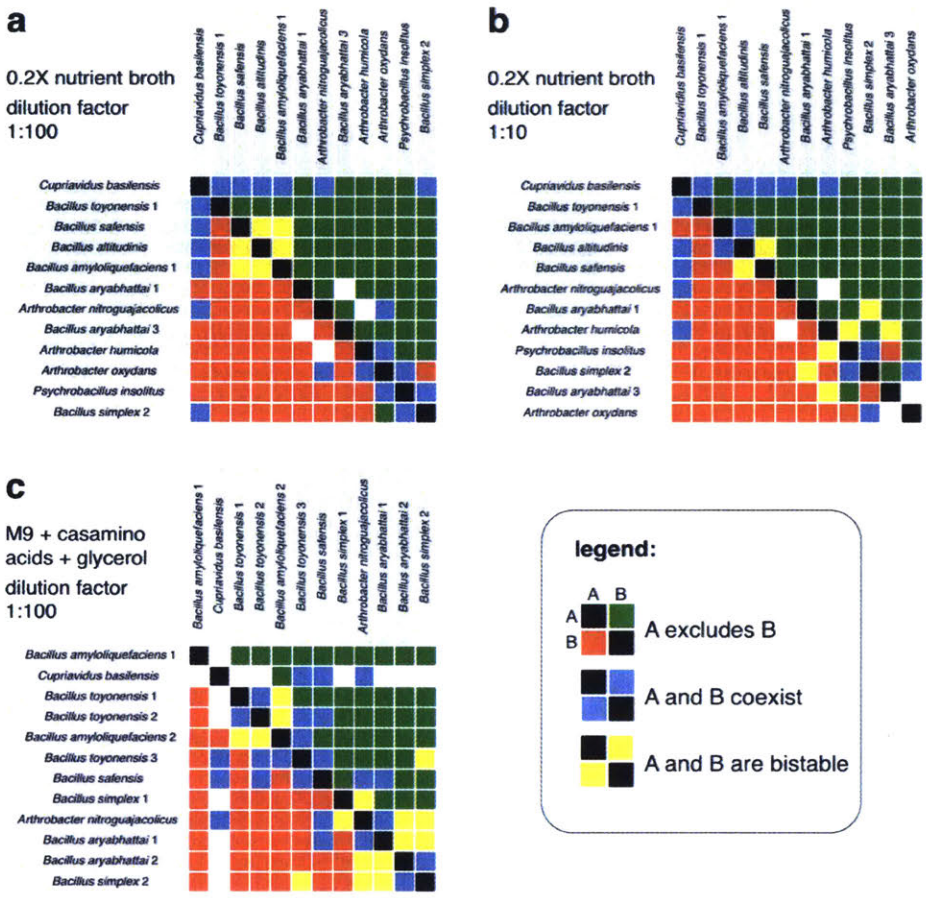

Supplementary Figure 2.2. The hierarchical network structure was reproduced across multiple environments. Subsets of 12 soil bacterial strains were competed in all pairwise combinations from two initial starting fractions (95%/5% and 5%/95% Strain A/Strain B) for five rounds of batch culture. Experiments were carried out in one of two growth media (either **a**, **b**, 0.2X nutrient broth or **c**, 1X M9 + 0.2% casamino acids + 0.4% glycerol) and at one of two daily dilution rates (either **a**, **c**, 1:100 or **b**, 1:10). After five successive growth-dilution cycles, cultures were plated on nutrient agar and the relative abundance of each strain was estimated by counting colonies. Under all environmental conditions tested, the resulting pairwise interaction network was significantly more hierarchical than the corresponding randomized interaction network ($p < 10^{-6}$ for all cases).

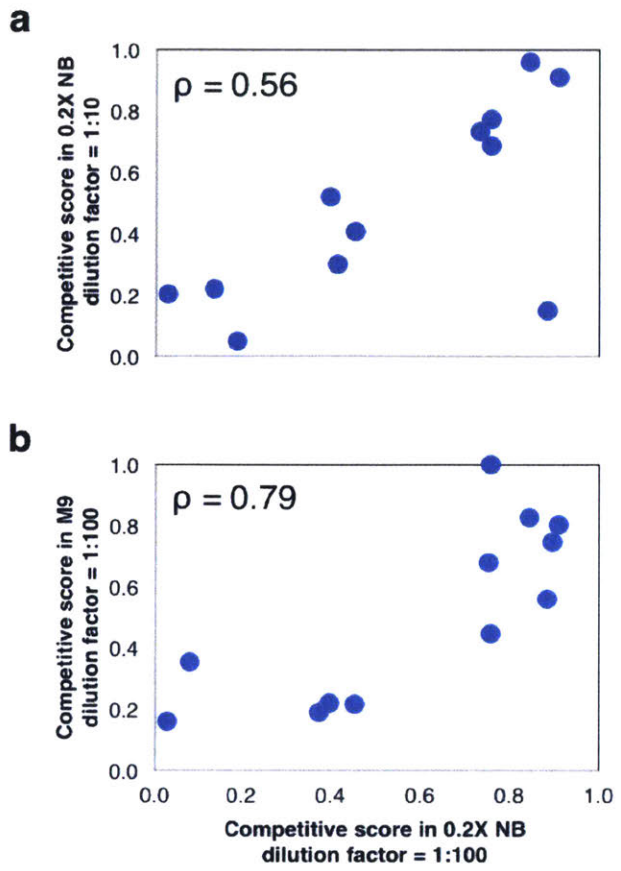

Supplementary Figure 2.3. Competitive performance was correlated across environments. Competitive score in the primary environment (0.2X nutrient broth, dilution factor = 1:100) versus: **a**, 0.2X nutrient broth, dilution factor = 1:10. **b**, M9 + 0.2% casamino acids + 0.4% glycerol, dilution factor = 1:100. In both comparisons, competitive performance in the primary environment was positively correlated with performance in the alternate environment. Experiments were performed as described in Supplementary Fig. 2.2.

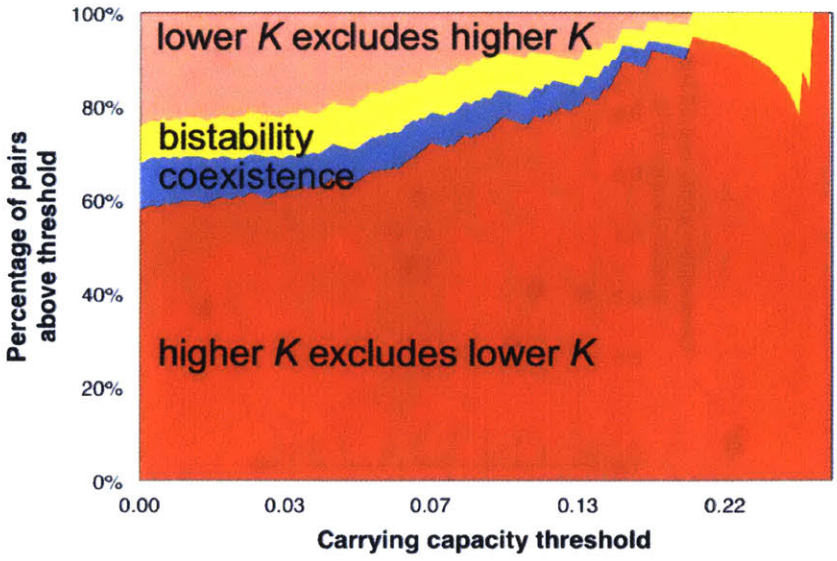

Supplementary Figure 2.4. The likelihood of exclusion increases with larger carrying capacity advantages. On average, we found that a strain is more likely to prevail in competition if it has a large carrying capacity advantage relative to the competitor. Overall, we found that the strain with the higher carrying capacity excludes the strain with the lower carrying capacity in ~59% of pairs. However, in a significant minority of cases (~23%), the low *K* strain excludes the high *K* strain. As capacity threshold increases, the likelihood of coexistence and exclusion of the high *K* strain both decrease.

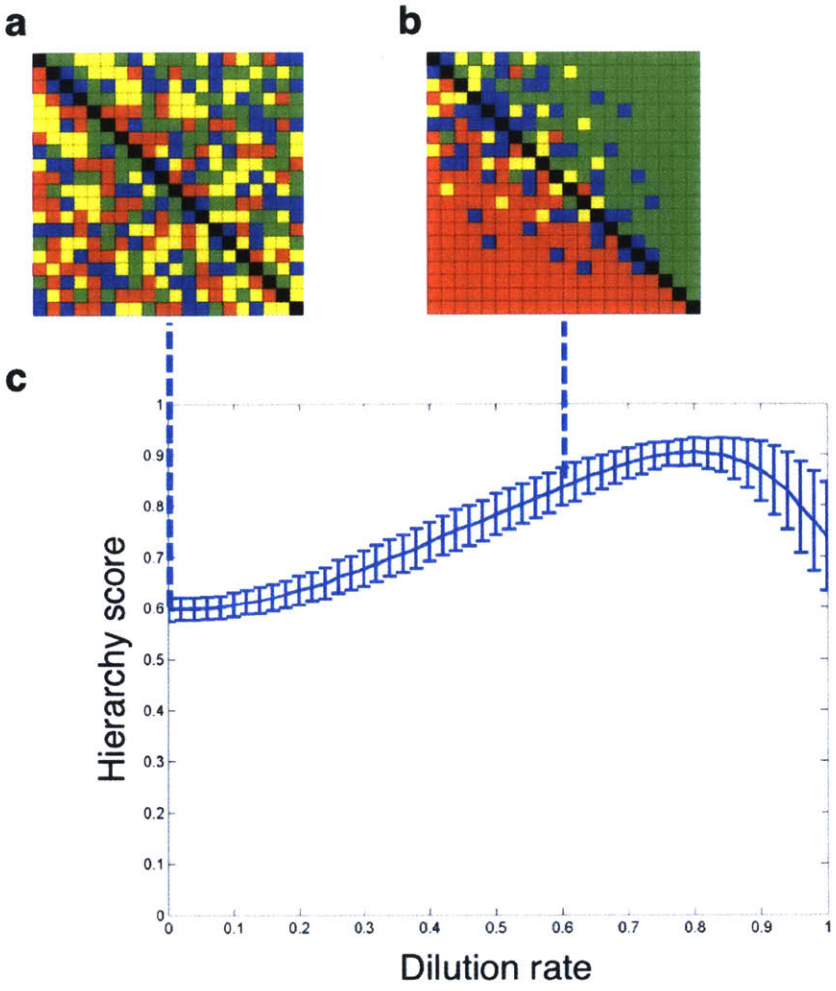

Supplementary Figure 2.5. Simulations suggest that differences in growth rate may result in increasing degrees of competitive hierarchy as the death rate increases. We employed a two-species generalized Lotka-Volterra (gLV) model to simulate pairwise interactions:

$$\frac{dx_i}{dt} = r_i x_i (1 - \sum_{j=1}^{n} \alpha_{ji} x_j) - \delta x_i$$

where x_i is the abundance of species i, r_i is the intrinsic growth rate of species i, α_{ji} is the interaction coefficient representing the effect of species j on the growth of species i, and δ is the death rate. **a**, **b**, simulated outcome matrices for $\delta = 0$ (**a**) and $\delta = 0.6$ (**b**). Intrinsic growth rates were sampled from a gaussian distribution with mean 1 and standard deviation 0.2. Interaction coefficients were sampled from a Gaussian distribution with mean 1 and standard deviation 0.3. Outcomes are color coded as in Fig. 2.2d and Supplementary Fig. 2.3a-c. **c**, dilution rates were varied between 0 and 1, with randomly assigned growth rates and interaction coefficients sampled from the distributions used to generate **a** and **b**. Data points represent the mean +/- 1 s.d. of 100 independent simulations.

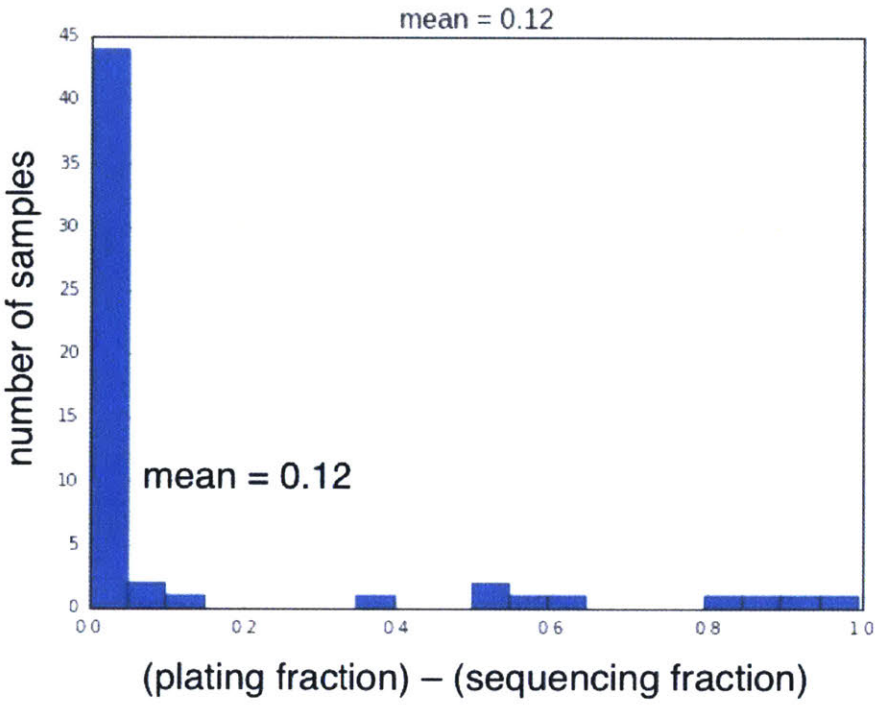

Supplementary Figure 2.6. Next-generation sequencing of representative co-cultures supports the relative abundance estimates determined via plating. In order to validate our method for estimating final species fractions, we amplified and sequenced the 16S rRNA gene from 56 randomly selected co-cultures at the end of the 5-day experiment. We estimated the relative abundance of each strain via sequencing and via plating. Shown above is a histogram of the difference between these two estimates. Out of these samples, three contained significant numbers of reads aligning to a species that is not in our collection, which we consider to be a contaminant. If the contaminated samples are excluded, the mean error is reduced to 0.11. Other sources of error include low colony counts for certain samples.

Supplementary Table 2.1. Summary of strains used.

strain	*r*	*K*	competitive score
Arthrobacter nitroguajacolicus	4.74×10^{-3}	0.202	0.396
Arthrobacter oxydans	2.51×10^{-3}	0.203	0.188
Arthrobacter humicola	3.52×10^{-3}	0.211	0.414
Cupriavidus basilensis	5.36×10^{-3}	0.196	0.844
Paenibacillus cellulositrophicus	n/a*	0.143	0.319
Psychrobacillus insolitus	2.24×10^{-3}	0.062	0.132
Rummeliibacillus pycnus	4.25×10^{-3}	0.153	0.361
Bacillus simplex 1	n/a*	0.051	0.028
Bacillus simplex 2	n/a*	0.092	0.079
Bacillus aryabhattai 1	1.37×10^{-2}	0.135	0.453
Bacillus aryabhattai 2	6.84×10^{-3}	0.127	0.374
Bacillus aryabhattai 3	4.74×10^{-3}	0.050	0.240
Bacillus flexus	4.56×10^{-3}	0.142	0.527
Bacillus toyonensis 1	6.84×10^{-3}	0.339	0.909
Bacillus toyonensis 2	7.25×10^{-3}	0.374	0.896
Bacillus toyonensis 3	6.48×10^{-3}	0.374	0.884
Bacillus amyloliquefaciens 1	5.13×10^{-3}	0.058	0.758
Bacillus amyloliquefaciens 2	5.60×10^{-3}	0.072	0.752
Bacillus altitudinis	5.87×10^{-3}	0.145	0.730
Bacillus safensis	6.16×10^{-3}	0.168	0.756

*Never reached threshold OD_{600}.

CHAPTER THREE

Community structure follows simple assembly rules in microbial microcosms

by Jonathan Friedman, Logan M. Higgins, and Jeff Gore

This chapter is presented, with minor changes, as it originally appeared in *Nature Ecology & Evolution* **1,** 0109 (2017).

3.1. Overview

Virtually every environment on Earth is teeming with microbial life, from the human digestive tract to hydrothermal vents, miles beneath the ocean's surface. These microbes are vital components of natural ecosystems: microbial activity drives Earth's biogeochemical cycles[50], fertilizes crops[51], and directly influences human health and well-being[52]. These functions are typically performed not by a single species, but rather by a diverse community composed of numerous interacting species. For example, there is a growing realization that numerous human illnesses, such as inflammatory bowel disease, are associated with an altered microbial community, rather than with any single pathogen[53]. The ability to predict the structure of these complex, multispecies communities is crucial for understanding how such communities form and function, managing natural communities, and rationally designing functional communities *de novo*[54,55,56].

Modeling and predicting microbial community structure is often pursued using bottom-up approaches that assume that species interact in a pairwise manner[57,58,59,60]. However, pair interactions may be modulated by the presence of additional species[61,62], an effect that can significantly alter community structure[63] and may be common in microbial communities[64]. While it has been shown that such models can provide a reasonable fit to sequencing data of intestinal microbiomes[65,66], their predictive power remains uncertain, as it has rarely been directly tested experimentally (refs [67,68] are notable exceptions).

Current approaches to modeling microbial communities commonly employ a specific parametric model, such as the generalized Lotka-Volterra (gLV) model[69,70,71]. Generating predictions from

such models requires fitting a large number of parameter values from empirical data, which is often challenging and prone to over-fitting. In addition, the exact form of the interactions needs to be assumed, and a failure of the model can reflect a misspecification of the type of pairwise interaction, rather than the presence of higher-order interactions[72].

Here we take an alternative approach in which qualitative information regarding the survival of species in competitions between small sets of species (e.g., pairwise competitions) is used to predict survival in more diverse multispecies competitions (Fig. 3.1). While this approach forgoes the ability to predict exact species abundances, it does not require specifying and parameterizing the exact form of interactions. Therefore, it is robust to model misspecification, and requires only survival data, which can be more readily obtained than exact parameter values.

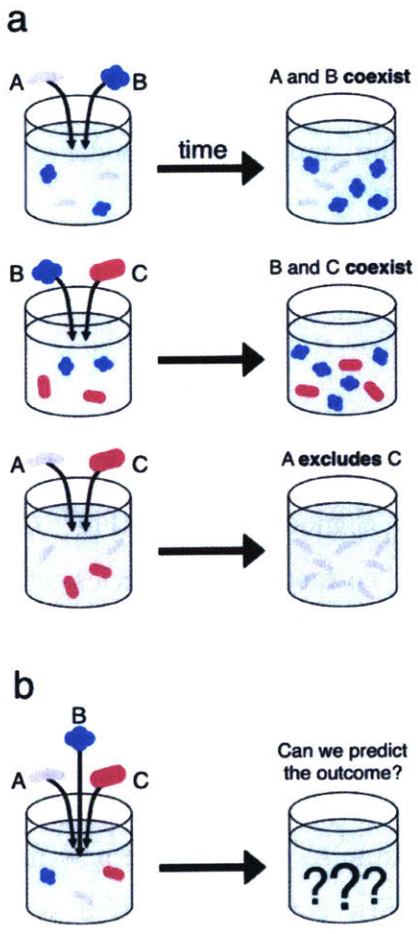

Figure 3.1. A bottom-up approach to predicting community composition from qualitative competitive outcomes. a,b, Qualitative information regarding the survival of species in

competitions among small sets of species, such as pairwise competitions (**a**), is used to predict survival in more diverse multispecies competitions, such as trio competitions (**b**). The particular pairwise outcomes illustrated here reflect the true outcomes observed experimentally in one set of three species (see Fig. 3.3b).

Intuitively, competitions typically result in the survival of a set of coexisting species, which cannot be invaded by any of the species that went extinct during the competition. To identify sets of species that are expected to coexist and exclude additional species, we first use the outcomes of pairwise competitions. We propose the following assembly rule: in a multispecies competition, species that all coexist with each other in pairs will survive, whereas species which are excluded by any of the surviving species will go extinct. This rule formalizes an intuitive expectation regarding how communities may assemble, and can be used to systemically predict community structure from pairwise outcomes (Methods and Supplementary Fig. 3.1). Importantly, the rule predicts the likely outcomes of competition, rather than the only possible ones. For example, for limited parameter values, even the simple gLV model can generate outcomes that are inconsistent with this assembly rule[73].

3.2. Results

To directly assess the predictive power of this approach, we used a set of eight heterotrophic soil-dwelling bacterial species as a model system (Fig. 3.2a and Methods). Competition experiments were performed by co-inoculating species at varying initial fractions, and propagating them through five growth-dilution cycles (Supplementary Fig. 3.2). During each cycle, cells were cultured for 48 hours and then diluted by a factor of 1500 into fresh media, which corresponds to ~10.6 cellular divisions per growth cycle, and ~53 cellular divisions over the entire competition period. The overall competition time was chosen such that species extinctions would have sufficient time to occur, while new mutants would typically not have time to arise and spread. Community compositions were assessed by measuring the culture optical density (OD), as well as by plating on solid agar media and counting colonies, which are distinct for each species[74]. These two measurements quantify the overall abundance of microbes

in the community, and the relative abundances of individual species, respectively. All experiments were done in duplicate.

Pairwise competitions resulted in stable coexistence or competitive exclusion of one of the species. We performed competitions between all species pairs and found that in the majority of the pairs (19/28 = 68%, Fig. 3.2b) both species could invade each other, and thus stably coexisted. In the remaining pairs (9/28 = 32%) competitive exclusion occurred, where only one species could invade the other (time trajectories from one coexisting pair and one pair where exclusion occurs are shown in Fig. 3.2c. Outcomes for all pairs are shown in Fig. 3.2d). Species' growth rate in monoculture was correlated with their average competitive ability, but, in line with previous reports[75], it could not predict well the outcome of specific pair competitions (Supplementary Fig. 3.3).

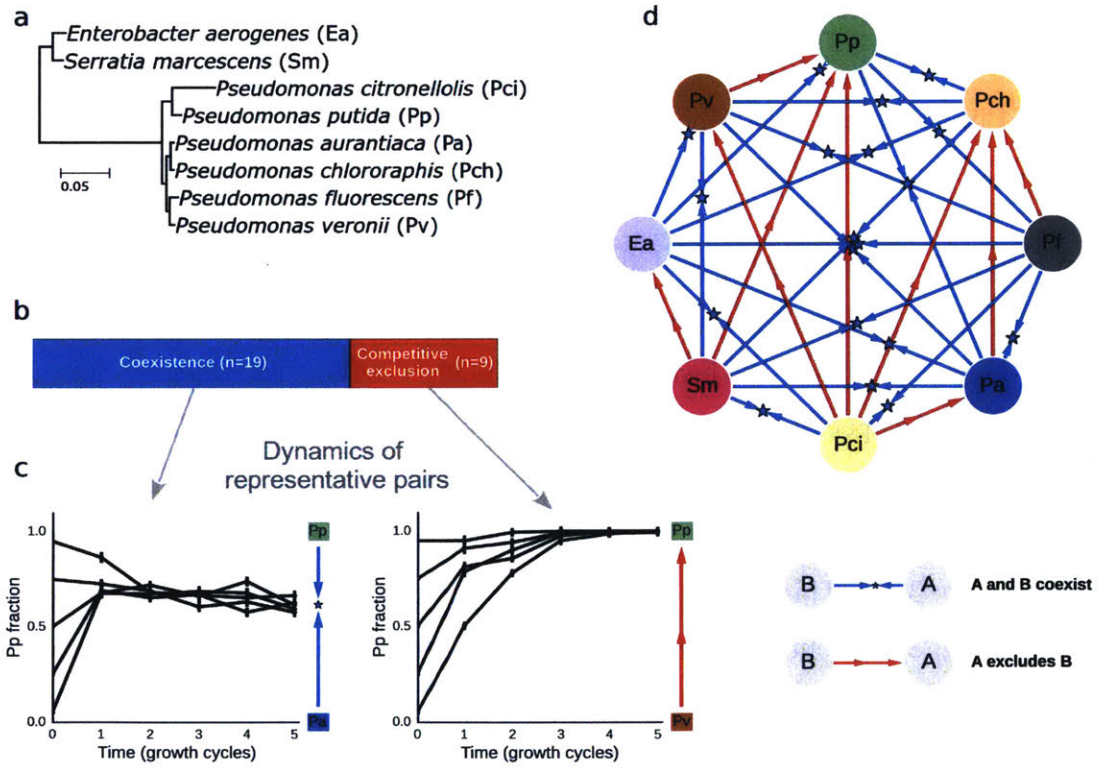

Figure 3.2. Pairwise competitions resulted in stable coexistence or competitive exclusion. a, Phylogenetic tree of the set of eight species used in this study. The tree is based on the full 16S gene and the branch lengths indicate the number of substitutions per base pair. **b,** Coexistence was observed for 19 of the 28 pairs, whereas competitive exclusion was observed for 9 of the 28

pairs. **c**, Changes in relative abundance over time in one pair where competitive exclusion occurred and one coexisting pair. The *y* axis indicates the fraction of one of the competing species. In the exclusion example (right panel), the species fraction increased for all initial conditions, resulting in the exclusion of the competitor. In contrast, in the coexistence case (left panel), fractions converged to an intermediate value and both species were found at the end of the competition. Error bars represent the standard deviation of the posterior beta distribution of the fractions, based on colony counts averaged across replicates. **d**, Network diagram of the outcomes of all pairwise competitions.

Next, we measured the outcome of competition between all 56 three-species combinations. These competitions typically resulted in a stable community whose composition was independent of the starting fractions (Supplementary Table 3.1). However, 2 of the 56 trios displayed inconsistent results with high variability between replicates. This variability likely resulted from rapid evolutionary changes that occurred during the competition (Supplementary Fig. 3.4). All but one of the other trio competitions resulted in stable communities with a single outcome, independent of starting conditions. This raises the question of whether this unique outcome could be predicted based upon the experimentally observed outcomes of the pairwise competitions.

Trios were grouped by the topology of their pairwise outcome network, which was used to predict their competitive outcomes. The most common topology involved two coexisting pairs, and a pair where competitive exclusion occurs (30/56 = 54%). To illustrate this scenario, consider a set of three species, labeled A, B, and C, where species A and C coexist with B in pairwise competitions, whereas C is excluded when competing with A. In this case, our proposed assembly rule predicts that the trio competition will result in the survival of species A and B, and exclusion of C (Fig. 3.3a**)**. This predicted outcome occurred for a majority of the experimentally observed trios (Fig. 3.3b), but some trio competitions resulted in less intuitive outcomes (Fig. 3.3c). For example, one of the 30 trios with this topology led to the extinction of A and the coexistence of B and C (Fig. 3.3c). The experimentally observed outcomes of competition in this trio topology highlights that our simple assembly rule typically works, and the failures provide a sense of alternative outcomes that are possible given the same underlying topology of pairwise outcomes. Unpredicted outcomes may occur due to several mechanisms, which are discussed in Section 3.3.

Another frequent topology was coexistence among all three species pairs (15/56 = 27%), in which case none of the species is predicted to be excluded in the trio competition (Fig. 3.3d). Such trio competitions resulted either in coexistence of all three species, as predicted by our assembly rule (Fig. 3.3e), or in the exclusion of one of the species (Fig. 3.3f). Overall, 5 different trio layouts and 11 competitive outcomes have been observed (Fig. 3.3g-k). Notably, all observed trio outcomes across all topologies can be generated from simple pairwise interactions, including the outcomes which were not correctly predicted by our assembly rule[73]. An incorrect prediction of our simple assembly rule is therefore not necessarily caused by higher-order interactions.

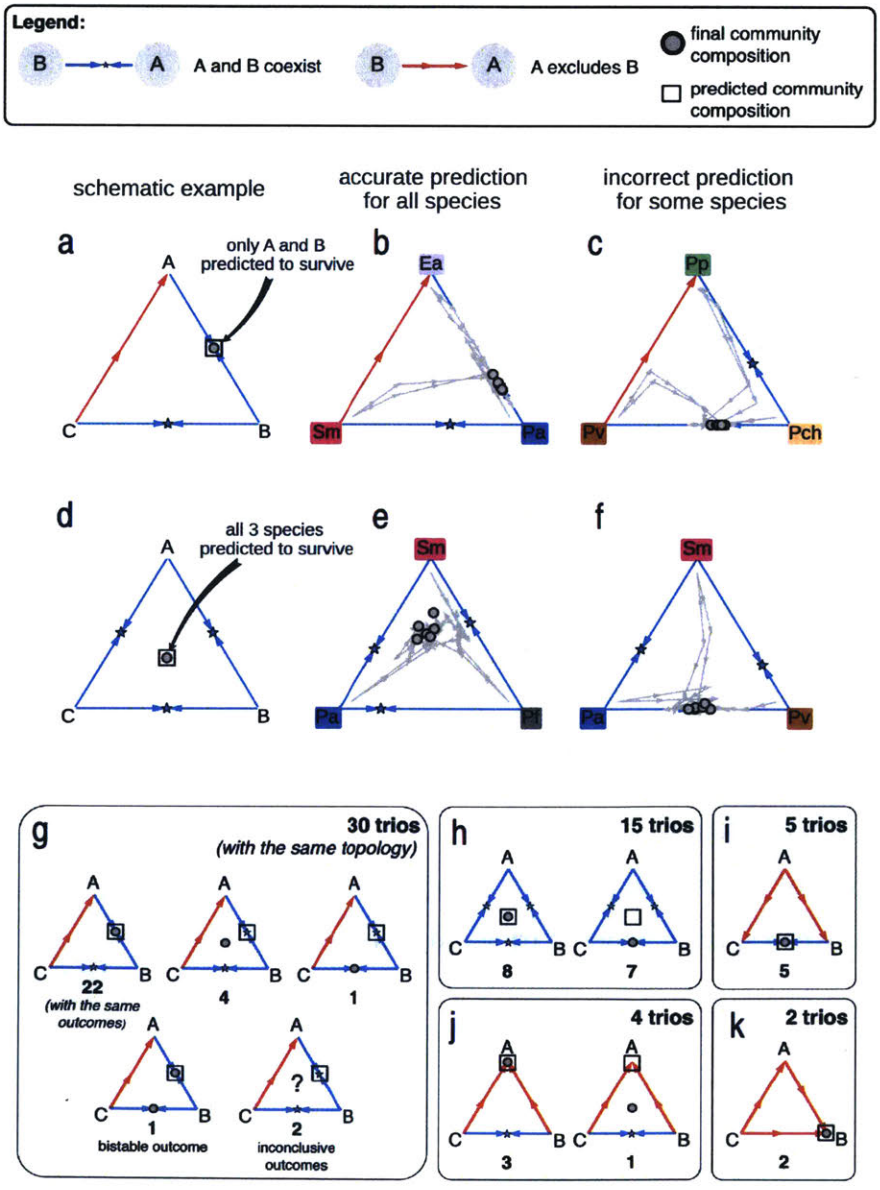

Figure 3.3. Observed and predicted outcomes of trio competitions. Changes in species fraction were measured over time for several trio competitions. **a-c**, Trios involving two coexisting pairs and one pair where competitive exclusion occurs. In these plots, each triangle is a simplex denoting the fractions of the three competing species. The simplex vertices correspond to a community composed solely of a single species, whereas edges correspond to a two-species mixture. The edges thus denote the outcomes of pair competitions, which were performed separately. Trajectories (grey arrows) begin at different initial compositions, and connect the species fractions measured at the end of each growth cycle. Dots mark the final community compositions. **a**, Schematic example, showing that only species A and B are predicted to coexist for this pattern of pairwise outcomes. **b**, Example of a trio competition which resulted in the predicted outcome. **c**, An example of an unpredicted outcome. **d-f**, Similar to **a-c**, but for trios where all species coexist in pairs. **g-k**, All trio layouts and outcomes, grouped by the topology of the pairwise outcome network. With the exception of one trio, all trio competitions resulted in a unique outcome. Dots denote the final community composition (not exact species fractions, but rather species survivals). One trio displayed bistability, which is indicated by two dots representing the two possible outcomes. Two trios displayed inconsistent results with high variability between replicates, which is indicated by a question mark.

Overall, survival in three-species competitions was well predicted by pairwise outcomes. The assembly rule predicted species survival across all the three-way competitions with an 89.5% accuracy (Fig. 3.4a), where accuracy is defined as the fraction of species whose survival was correctly predicted. To get a sense of how the observed accuracy compares to the accuracy attainable when pairwise outcomes are not known, as a null model, we considered the case where the only information available is the average probability that a species will survive in a trio competition (note that this probability is not assumed to be available in our simple assembly rule). Using this information, trio outcomes could only be predicted with a 72% accuracy (Fig. 3.4a and Methods). We further compared the observed accuracy to the accuracy expected when species interact solely in a pairwise manner, according to the gLV equations with a random interaction matrix (Methods). We found that the observed accuracy is consistent with the accuracy obtained in simulations of competitions that parallel our experimental setup ($p=0.29$, Fig. 3.4b). Survival of species in pairwise competition is therefore surprisingly effective in predicting survival when species undergo trio competition.

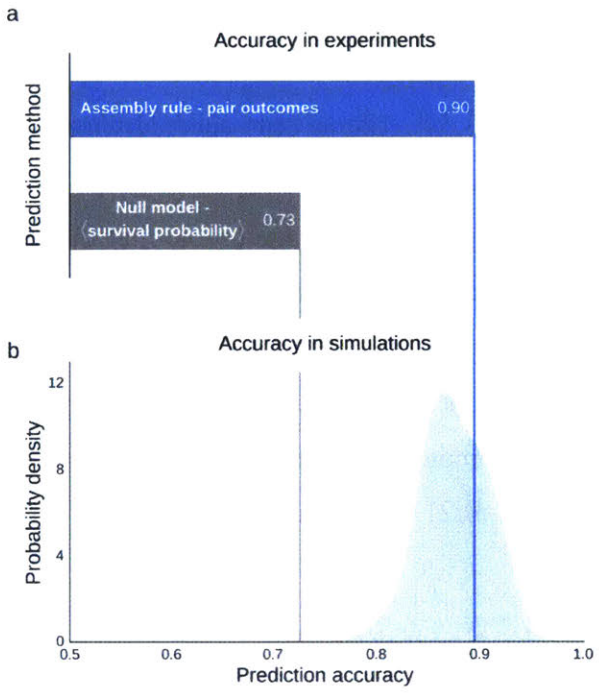

Figure 3.4. Survival in trio competitions is well predicted by pairwise outcomes. a, Prediction accuracy of the assembly rule and the null model, where predictions are made solely based on the average probability that species survive in trio competitions. **b**, The distribution of accuracies of prediction made using the assembly rule from gLV simulations that mirror our experimental design. The experimentally observed accuracy is consistent with those found in the simulations.

Nonetheless, there are exceptional cases where qualitative pairwise outcomes are not sufficient to predict competitive outcomes of trio competitions. Accounting for such unexpected trio outcomes may improve prediction accuracy for competitions involving a larger set of species. We encode unexpected trio outcomes by creating effective modified pairwise outcomes, which replace the original outcomes in the presence of an additional species. For example, competitive exclusion will be modified to an effective coexistence when two species coexist in the presence of a third species despite one of them being excluded from the pair competition. The effective, modified outcomes can be used to make predictions using the assembly rule as before (Methods and Supplementary Fig. 3.1). By accounting for unexpected trio outcomes, the assembly rule extends our intuition, and predicts community structure in the presence of potentially complex interactions.

The ability of the assembly rule to predict the outcomes of more diverse competitions was assessed by measuring survival in competitions among all seven-species combinations, as well as the full set of eight species (Fig. 3.5a). Using only the pairwise outcomes, survival in these competitions could only be predicted with an accuracy of 62.5%, which is barely higher than the 61% accuracy obtained when using only the average probability that a species will survive these competitions (Fig. 3.5b). A considerably improved prediction accuracy of 86% was achieved by incorporating information regarding the trio outcomes (Fig. 3.5b). As in the trio competitions, the observed accuracies are consistent with those obtained in gLV simulations that parallel the experimental setup, both when predicting using pairwise outcomes alone (p=0.53), or in combination with trio outcomes (p=0.21, Fig. 3.5c).

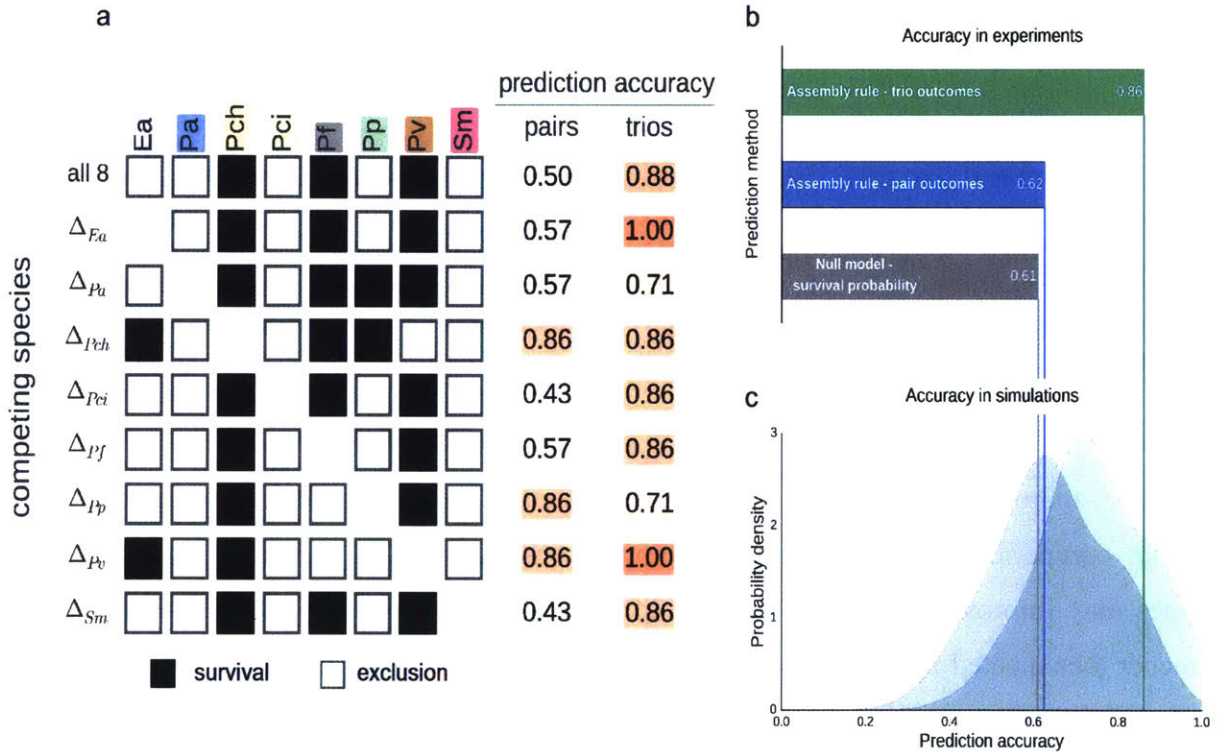

Figure 3.5. Predicting survival in more diverse competition required incorporating the outcomes of the trio competitions. a, Species survival when competing all eight species, and all sets of seven species. White and black boxes indicate survival and extinction, respectively. Survival is predicted either using only pair outcomes, or using both pair and trio outcomes. **b**, Prediction accuracy of the null model and the assembly rule, using either pair outcomes only, or pair and trio outcomes. **c**, The distribution of accuracies of prediction made using the assembly rule from gLV simulations that mirror our experimental design. In these simulations, predictions

were made using either pair outcomes only, or pair and trio outcomes. In both cases, the experimentally observed accuracies are consistent with those found in the simulations.

3.3. Discussion

Our assembly rule makes predictions that match our intuition, but there are several conditions under which these predictions may be inaccurate. First, community structure can be influenced by initial species abundances[76], as has recently been demonstrated in pairwise competitions between bacteria of the genus *Streptomyces*[77]. Our assembly rule may be able to correctly predict the existence of multiple stable states, as it identifies all putative sets of coexisting, non-invasible species in a given species combination. However, we did not have sufficient data to evaluate the rule's accuracy in such cases, as multi-stability was observed in only one of all our competition experiments.

Complex ecological dynamics, such as oscillations and chaos, can also have a significant impact on species survival[78,79], making it difficult to predict the community structure. These dynamics can occur even in simple communities containing only a few interacting species. For example, oscillatory dynamics occur in gLV models of competition between as few as three species[73], and have been experimentally observed in a cross-protection mutualism between a pair of bacterial strains[80]. In contrast, our competitions predominantly resulted in a unique and stable final community. This occurred despite the fact that we observed complex inter-species interactions involving interference competition and facilitation (Supplementary Fig. 3.4). These results indicate that complex ecological dynamics may in fact be rare, though it remains to be seen whether they become more prevalent in more diverse assemblages. Relatedly, prediction is challenging in the presence of competitive cycles (e.g. "Rock-Paper-Scissors" interactions), which often lead to oscillatory dynamics, and are thought to increase species survival and community diversity[81,82]. Such non-hierarchical relationships are absent from our competitive network, and thus their effect cannot be evaluated here.

In the absence of multi-stability or complex dynamics, our approach may still fail when competitive outcomes do not provide sufficient information regarding the interspecies interactions. This could be due to higher-order interactions, which only manifest in the presence

of additional species, or because only qualitative information regarding survival is utilized. The observed accuracy of the assembly rule was consistent with the one found in gLV simulations, but this does not necessarily indicate that our species interact in a linear, pairwise fashion. In fact, fitting the gLV model directly to our pairwise data does not improve predictability (Supplementary Fig. 3.6). Determining whether, in any particular competition, predictions fail due to insufficient information regarding the strength of linear interactions, non-linear interactions, or higher-order interactions will require more detailed measurements.

Controlling and designing microbial communities has numerous important application areas ranging from probiotic therapeutics, to bioremediation and biomanufacturing[54]. The ability to predict what community will be formed by a given set of species is crucial for determining how extinctions and invasions will affect existing communities, and for engineering desired communities. Our results suggest that, when measured in the same environment, community structure can be predicted from the outcomes of competitions among small sets of species, demonstrating the feasibility of a bottom-up approach to understanding and predicting community structure. While these results are encouraging, they were obtained using a small set of closely related species in well-controlled laboratory settings. It remains to be seen to what extent these results hold in other systems and in more natural settings, involving more diverse assemblages which contain additional trophic levels, in the presence of spatial structure, and over evolutionary time scales.

3.4. Methods

Species and media. The eight soil bacterial species used in this study are *Enterobacter aerogenes* (Ea, ATCC#13048), *Pseudomonas aurantiaca* (Pa, ATCC#33663), *Pseudomonas chlororaphis* (Pch, ATCC#9446), *Pseudomonas citronellolis* (Pci, ATCC#13674), *Pseudomonas fluorescens* (ATCC#13525), *Pseudomonas putida* (ATCC#12633), *Pseudomonas veronii* (ATCC#700474), and *Serratia marcescens* (Sm, ATCC#13880). All species were obtained from ATCC. The base growth media was M9 minimal media[25], which contained 1X M9 salts (Sigma Aldrich, M6030), 2 mM MgSO4, 0.1 mM CaCl2, 1X trace metals (Teknova, T1001). For the final growth media, the base media was supplemented with 1.6 mM galacturonic acid and 3.3

mM serine as carbon sources, which correspond to 10 mM of carbon for each of these substrates. These carbon sources were chosen from a set of carbon sources commonly used to characterize soil microbes (Biolog, EcoPlate) to ensure that each of the eight species survives in monoculture. Nutrient broth (0.3% yeast extract, 0.5% peptone) was used for initial inoculation and growth prior to experiment. Plating was done on 10cm Petri dishes containing 25 mL nutrient agar (nutrient broth with 1.5% agar added).

Competition experiments. Frozen stocks of individual species were streaked out on nutrient agar Petri plates, grown at room temperature for 48 hr, and then stored at 4 °C for up to 2 weeks. Prior to competition experiments, single colonies were picked and each species was grown separately in 50mL Falcon tubes, first in 5ml nutrient broth for 24 hr and next in 5 ml of the experimental M9 media for 48 hr. During the competition experiments, cultures were grown in Falcon flat-bottom 96-well plates (BD Biosciences), with each well containing a 150 µl culture. Plates were incubated at 25 °C without shaking, and were covered with a lid and wrapped in Parafilm. For each growth-dilution cycle, the cultures were incubated for 48 hr and then serially diluted into fresh growth media by a factor of 1500.

Initial species mixtures were performed by diluting each species separately to an optical density (OD) of $3*10^{-4}$. Different species were then mixed by volume to the desired composition. This mixture was further diluted to an OD of 10^{-4}, from which all competitions were initialized. For each set of competing species, competitions were conducted from all the initial conditions in which each species was present at 5%, except for one more abundant species. For example, for each species pair there were 2 initial conditions with one species at 95% and the other at 5%, whereas for the 8 species competition there were 8 initial conditions each with a different species at 65% and the rest at 5%. For a few species pairs (Fig. 3.2a-b), we conducted additional competitions starting at more initial conditions. All experiments were done in duplicate.

Measurement of cell density and species fractions. Cell densities were assessed by measuring optical density at 600 nm using a Varioskan Flash plate reader. Relative abundances were measured by plating on nutrient agar plates. Each culture was diluted by a factor between 10^5 and 10^6 in phosphate-buffered saline, depending on the culture's OD. For each diluted culture, 75 µl were plated onto an agar plate. Colonies were counted after 48 hr incubation at room

temperature. A median number of 85 colonies per plate were counted. To determine species extinction in competition between a given set of species, we combined all replicates and initial conditions from that competition, and classified as extinct any species whose median abundance was less than 1%, which is just above our limit of detection.

Assembly rule predictions and accuracy. For any group of competing species, predictions were made by considering all possible competitive outcomes (e.g. survival of any single species, any species pair, etc.). Outcomes that were consistent with our assembly rule were those that were predicted to be a possible outcome of the competition (Supplementary Fig. 3.1). For any given competition, there may be several such feasible outcomes, however a unique outcome was predicted for all our competition experiments.

Pairwise outcomes were modified using trio outcomes as following: Exclusion was replaced with coexistence for pairs that coexisted in the presence of any additional species. Coexistence was replaced with exclusion whenever a species went extinct in a trio competition with two species with which it coexisted when competed in isolation. Only modifications cause by the surviving species, or an invading species were considered. Therefore, a new set of modified pairwise outcomes was generated for each putative set of surviving species being evaluated.

The prediction accuracy was defined as the fraction of species whose survival was correctly predicted. When the assembly rule identified multiple possible outcomes, which occurred only in the gLV simulations, accuracy was averaged over all such feasible outcomes. Additionally, when the competitive outcome depended on the initial condition, accuracy was averaged across all initial conditions.

For reference, we computed the accuracy of predictions made based on the probability that a species will survive a competition between the same number of species. For example, for predicting trio outcomes, we used the proportion of species that survived, averaged across all trio competitions. Using this information, the highest accuracy would be achieved by predicting that all species survive in all competitions, if the average survival probability is > 0.5, and predicting that all species go extinct otherwise.

Simulated competitions. To assess the assembly rule's expected accuracy in a simple case in which species interact in a purely pairwise manner, we simulated competitions using the generalized Lotka-Volterra (gLV) dynamics:

$$\dot{x}_i = r_i x_i \left(1 - x_i + \sum_{i \neq j} \alpha_{ij} x_j \right),$$

where x_i is the density of species i (normalized to its carrying capacity), r_i is the species' intrinsic growth rate, and α_{ij} is the interaction strength between species i and j. For each simulation, we created a set of species with random interactions where the α_{ij} parameters were independently drawn from normal distribution with a mean of 0.6 and a standard deviation of 0.46. Results were insensitive to variations in growth rates, thus they were all set to 1 for simplicity. These parameters recapitulate the proportions of coexistence and competitive exclusion observed in our experiments, and yield a distribution of trio layouts similar to the one (Supplementary Fig. 3.7). The probability of generating bistable pairs in these simulations is low (~3.7%, corresponding to one bistable pair in a set of eight species), and we further excluded the bistable pairs that were occasionally generated by chance, since we had not observed any such pairs in the experiments.

The accuracy of the assembly rules in gLV systems was estimated by running simulations that parallel our experimental setup: A set of eight species with random interaction coefficients was generated, and the pairwise outcomes were determined according to their interaction strengths. These outcomes were used to generate predictions for the trio competitions using our assembly rule. Next, all three-species competitions were simulated with the same set of initial conditions used in the experiments. Finally, the predicted trio outcomes were compared to the simulation outcomes across all trios to determine the prediction accuracy. Thus, a single accuracy value was recorded for each set of eight simulated species. Similarly, for each simulated eight-species set, the pair and trio outcomes were used to generate predictions for the seven-species and eight-species competitions, and their accuracy was assessed by comparing them to the outcomes of simulated competitions. Prediction accuracy distributions were estimated using Gaussian kernel density estimation from the accuracy values of 100 simulated sets of eight species.

One-sided P-values evaluating the consistency of the experimentally observed accuracies with the simulation results were defined as the probability that a simulation would yield an accuracy which is at least as high as the experimentally observed one.

Code availability. An implementation of the assembly rule and the gLV simulations, as well as routines for evaluating the rule's accuracy are freely available online at: https://bitbucket.org/yonatanf/assembly-rule.

Data availability. The data that support the findings of this study are available from the corresponding authors upon reasonable request.

[50] Falkowski, P., Fenchel, T. & Delong, E. The microbial engines that drive Earth's biogeochemical cycles. *Science* **320,** 1034–9 (2008).

[51] Berendsen, R. L., Pieterse, C. M. & Bakker, P. A. The rhizosphere microbiome and plant health. *Trends Plant Sci.* **17,** 478–486 (2012).

[52] Flint, H. J., Scott, K. P., Louis, P. & Duncan, S. H. The role of the gut microbiota in nutrition and health. *Nat. Rev. Gastroenterol. Hepatol.* **9,** 577–589 (2012).

[53] Matsuoka, K. & Kanai, T. The gut microbiota and inflammatory bowel disease. *Semin. Immunopathol.* **37,** 47–55 (2015).

[54] Widder, S. *et al.* Challenges in microbial ecology: building predictive understanding of community function and dynamics. *ISME J.* **10,** 2557-2568 (2016).

[55] Großkopf, T. & Soyer, O. S. Synthetic microbial communities. *Curr. Opin. Microbiol.* **18,** 72–77 (2014).

[56] Fredrickson, J. K. Ecological communities by design. *Science* **348,** 1425-1427 (2015).

[57] Faust, K. & Raes, J. Microbial interactions: from networks to models. *Nat. Rev. Microbiol.* **10,** 538–550 (2012).

[58] Bucci, V. & Xavier, J. B. Towards Predictive Models of the Human Gut Microbiome. *J. Mol. Biol.* **426,** 3907–3916 (2014).

[59] Berry, D. & Widder, S. Deciphering microbial interactions and detecting keystone species with co-occurrence networks. *Front. Microbiol.* **5,** 219 (2014).

[60] Carrara, F., Giometto, A., Seymour, M., Rinaldo, A. & Altermatt, F. Inferring species interactions in ecological communities: a comparison of methods at different levels of complexity. *Methods Ecol. Evol.* **6,** 895-906 (2015).

[61] Billick, I. & Case, T. J. Higher Order Interactions in Ecological Communities: What Are They and How Can They be Detected? *Ecology* **75,** 1530–1543 (1994).

[62] Momeni, B. & Shou, W. The validity of pairwise models in predicting community dynamics. *bioRxiv* 60988 (2016). doi:10.1101/060988

[63] Wootton, J. T. The nature and consequences of indirect effects in ecological communities. *Annu. Rev. Ecol. Syst.* **25,** 443–466 (1994).

[64] Kelsic, E. D., Zhao, J., Vetsigian, K. & Kishony, R. Counteraction of antibiotic production and degradation stabilizes microbial communities. *Nature* **521,** 516-519 (2015).

[65] Stein, R. R. *et al.* Ecological Modeling from Time-Series Inference: Insight into Dynamics and Stability of Intestinal Microbiota. *PLOS Comput Biol* **9,** e1003388 (2013).

[66] Bucci, V. *et al.* MDSINE: Microbial Dynamical Systems INference Engine for microbiome time-series analyses. *Genome Biol.* **17,** 121 (2016).

[67] Vandermeer, J. H. The competitive structure of communities: an experimental approach with protozoa. *Ecology* **50,** 362–371 (1969).

[68] Dormann, C. F. & Roxburgh, S. H. Experimental evidence rejects pairwise modelling approach to coexistence in plant communities. *Proc. R. Soc. Lond. B Biol. Sci.* **272,** 1279–1285 (2005).

[69] Mounier, J. *et al.* Microbial Interactions within a Cheese Microbial Community. *Appl. Environ. Microbiol.* **74,** 172–181 (2008).

[70] Fisher, C. K. & Mehta, P. Identifying Keystone Species in the Human Gut Microbiome from Metagenomic Timeseries Using Sparse Linear Regression. *PLOS ONE* **9,** e102451 (2014).

[71] Marino, S., Baxter, N. T., Huffnagle, G. B., Petrosino, J. F. & Schloss, P. D. Mathematical modeling of primary succession of murine intestinal microbiota. *Proc. Natl. Acad. Sci.* **111,** 439–444 (2014).

[72] Case, T. J. & Bender, E. A. Testing for Higher Order Interactions. *Am. Nat.* **118,** 920–929 (1981).

[73] Zeeman, M. L. Hopf bifurcations in competitive three-dimensional Lotka–Volterra systems. *Dyn. Stab. Syst.* **8,** 189–216 (1993).

[74] Celiker, H. & Gore, J. Clustering in community structure across replicate ecosystems following a long-term bacterial evolution experiment. *Nat. Commun.* **5,** 4643 (2014).

[75] Concepción-Acevedo, J., Weiss, H. N., Chaudhry, W. N. & Levin, B. R. Malthusian Parameters as Estimators of the Fitness of Microbes: A Cautionary Tale about the Low Side of High Throughput. *PLOS ONE* **10,** e0126915 (2015).

[76] Fukami, T. Historical Contingency in Community Assembly: Integrating Niches, Species Pools, and Priority Effects. *Annu. Rev. Ecol. Evol. Syst.* **46,** 1–23 (2015).

[77] Wright, E. S. & Vetsigian, K. H. Inhibitory interactions promote frequent bistability among competing bacteria. *Nat. Commun.* **7,** 11274 (2016).

[78] Armstrong, R. A. & McGehee, R. Competitive Exclusion. *Am. Nat.* **115,** 151–170 (1980).

[79] Huisman, J. & Weissing, F. Biodiversity of plankton by species oscillations and chaos. *Nature* **402,** 407-410 (1999).

[80] Yurtsev, E. A., Conwill, A. & Gore, J. Oscillatory dynamics in a bacterial cross-protection mutualism. *Proc. Natl. Acad. Sci.* **113,** 6236–6241 (2016).

[81] Kerr, B., Riley, M. A., Feldman, M. W. & Bohannan, B. J. Local dispersal promotes biodiversity in a real-life game of rock–paper–scissors. *Nature* **418,** 171–174 (2002).

[82] Allesina, S. & Levine, J. A competitive network theory of species diversity. *Proc. Natl. Acad. Sci. USA* **108,** 5638-5642 (2011).

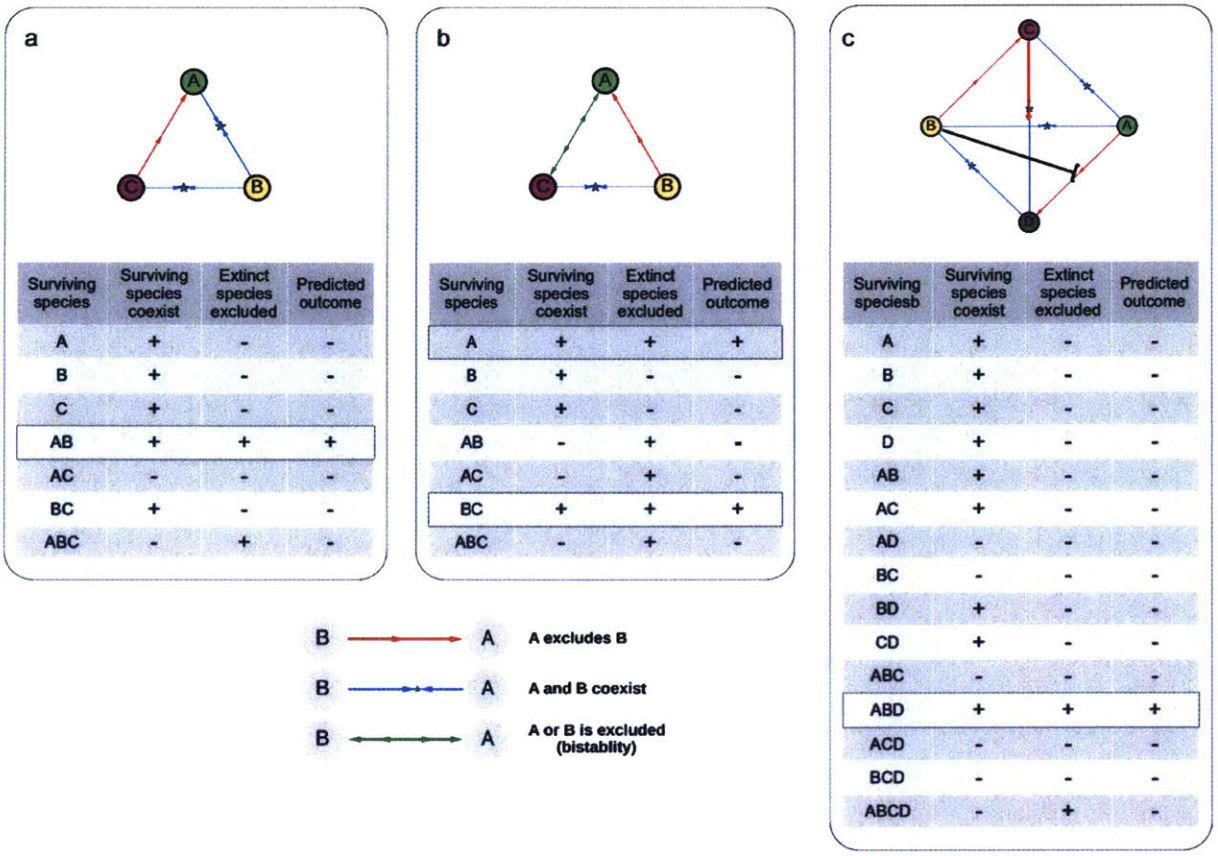

Supplementary Figure 3.1. Simple examples of applying the assembly rule. We consider three examples of competing species and their pairwise and trio (in panel **c**) competitive outcomes. In each example, we enumerate all possible candidate sets of surviving species. For each set, we denote whether all species within the set coexist, and whether all species not included in the set are excluded by at least one surviving species. Sets that fulfill both of these conditions are predicted to be feasible outcomes of the competition. **a**, The most common pattern of pairwise outcomes among three species observed experimentally. Species C is not expected to survive along with species A, and A and B are both predicted to survive, since they are not excluded by any other species. Therefore, in this simple case, the only predicted outcome is survival of A and B, and the exclusion of C. **b**, A trio involving a bistability between species A and C. This case is predicted to have two possible competitive outcomes: A being the sole survivor, since it excludes B and cannot be invaded by C; or exclusion of A and coexistence of B and C. The latter can be a stable outcome since A cannot invade in the presence of C. **c,** An example including unexpected trio outcomes. Species C is excluded in the trio ABC, despite coexisting with A and excluding B in pairwise competition. Additionally, species A survives in tro ABD despite being excluded by D in isolation. The only predicted outcome in this case is survival of A, B, and D, and exclusion of C. Survival of A, C, and D, and exclusion of B is not a predicted outcome since C, rather than B, is excluded in the presence of A.

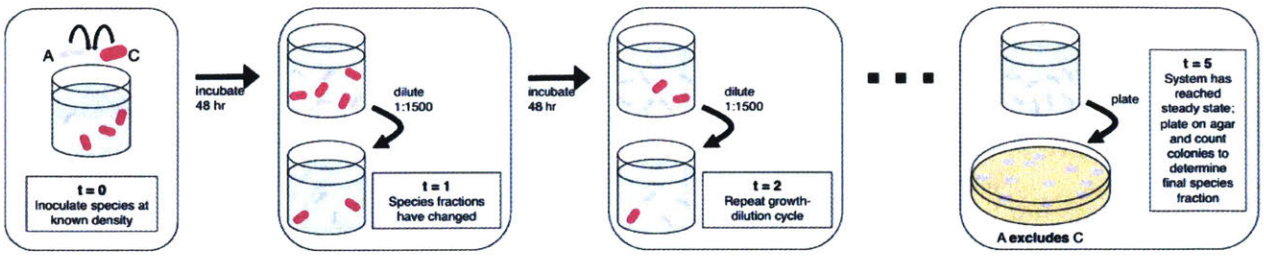

Supplementary Figure 3.2. Competition experiments were performed by co-inoculating species and propagating them through five growth-dilution cycles. During each cycle, cells were cultured for 48 hours and then diluted by a factor of 1500 into fresh M9 media supplemented with galacturonic acid and serine as sole carbon sources. Community compositions were assessed by measuring the culture optical density (OD), as well as by plating on solid agar media and counting colonies, which are distinct for each species. Community composition was quantified at the end of the fifth cycle for all competitions, or at the end of every cycle in cases where the dynamics of competitions were investigated (Fig. 3.2 **c**, Fig. 3.3 **b**,**c**,**e**,**f**).

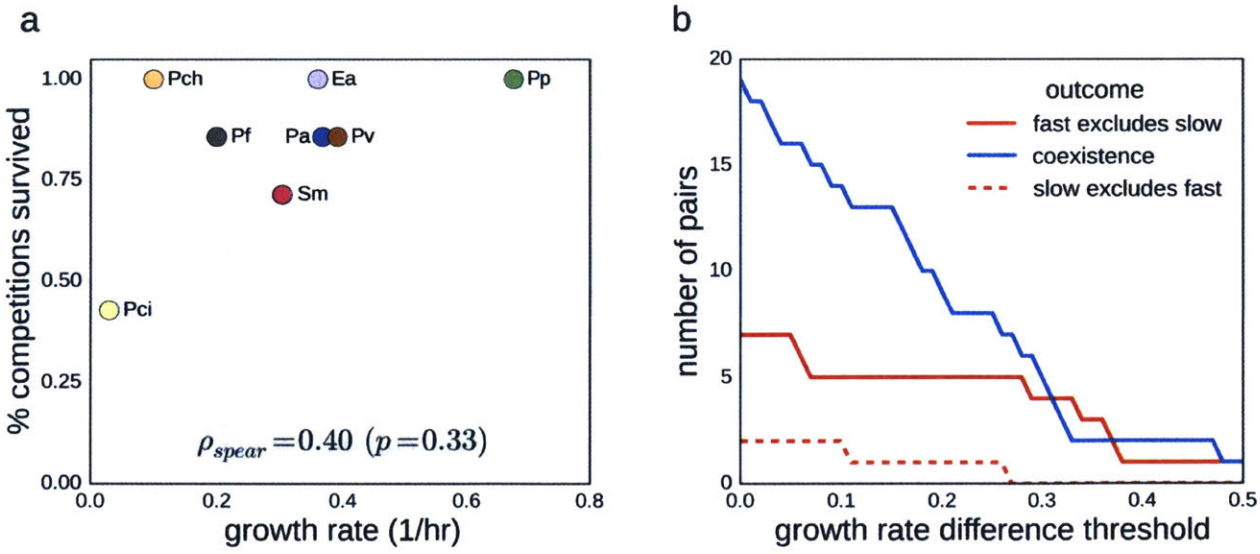

Supplementary Figure 3.3. Growth rate in monoculture is correlated with competitive ability, but does not predict pairwise competitive outcomes. a, Faster growing species tend to survive pairwise competitions more often than slow growers. **b**, The probability that a fast-growing species will exclude a slow-growing species in pairwise competition increased with the difference between their growth rates. Nonetheless, even pairs which had a big discrepancy in growth rates where roughly as likely to coexist as they were to result in exclusion of the slow grower. To estimate growth rates, growth curves were measured for each species in a Tecan Infinite 200 Pro plate reader. Growth rates were estimated as the exponential growth rate which corresponds to the measured time it took each species to reach a given optical density (10^{-2}) from a known initial density (~10^{-4}). These growth rates account for any initial lag time, or slower growth period, which may impact species' competitive performance.

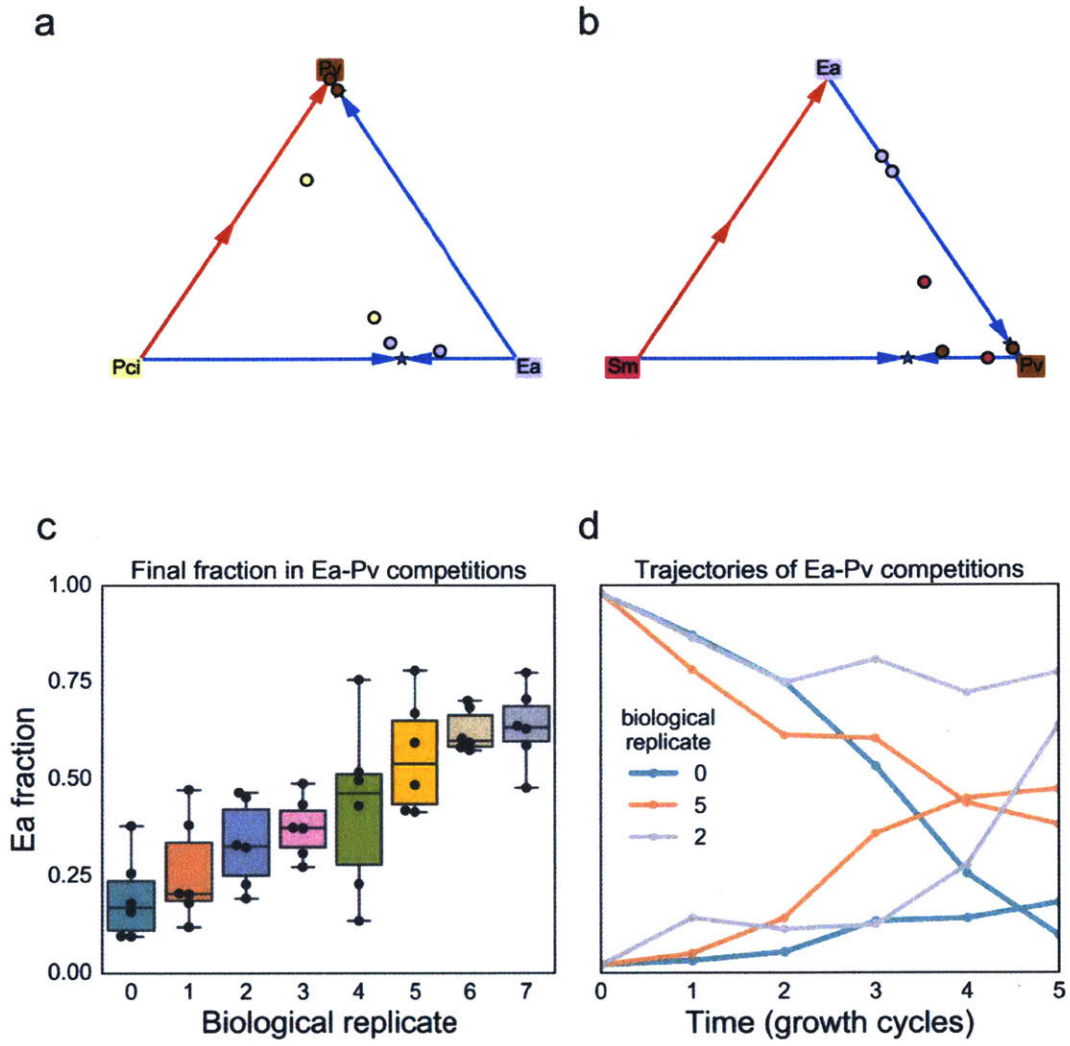

Supplementary Figure 3.4. Inconsistent trio outcomes are likely due to rapid evolution. a,b, In two trios, we observed high variability in competitive outcomes between initial conditions, as well as between replicates. Both of these cases involved a common pair of species: Ea-Pv. The triangle are simplex plots, with edges indicating the pairwise outcomes, and dots denoting the fractions of species at the end of competitions. Dot colors indicate the initial condition of the competition: at the beginning of competition, the species with the corresponding color was present at 90% of the total cell density, and the other two species were at 5% each. Competitions starting from each initial condition were done in duplicate. **c**, To test whether this variability could arise during the experiment, we performed additional competitions between Ea and Pv, involving eight biological replicates and six initial fractions for each replicate. For each biological replicate, a colony of each species was picked at the beginning of the experiment and grown in rich media and subsequently in the experimental media prior to the beginning of competitions (Methods). While all competitions resulted in the coexistence of both species, the coexistence fraction varied significantly. Most of this variability occurred across the biological replicates, potentially indicating adaptation during the growth prior to the beginning of competitions. **d**, Fraction trajectories for two initial conditions of three of the biological replicates, highlighting the variability between biological replicates.

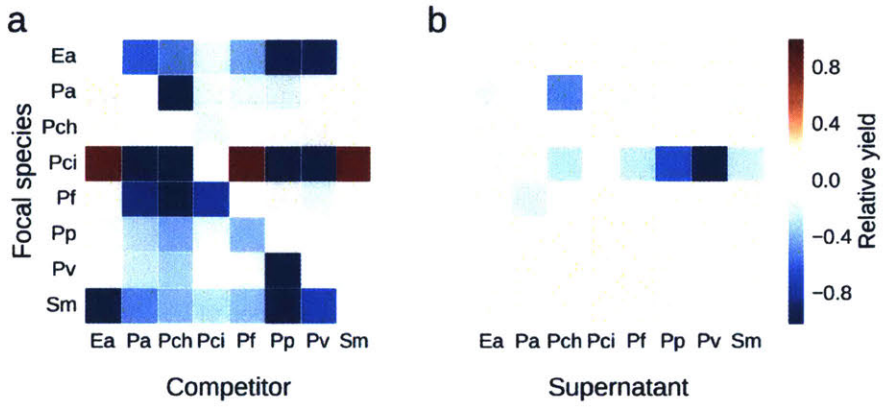

Supplementary Figure 3.5. Inter-species interactions included interference competition and facilitation. a, Several species grew to a higher density in the presence of an additional species than in monoculture. The impact of each competitor on each focal species was quantified by calculating its relative yield, defined as: (density in coculture - density in monoculture)/(density in coculture + density in monoculture). A negative relative yield indicates growth hindrance, whereas positive values indicated facilitation. **b**, Interference competition was detected by growing species on supernatant media in all pairwise combinations. Supernatant was obtained by filter sterilizing experimental media in which monocultures were grown for 48 hr. The supernatant media was composed of supernatant supplemented with carbon sources and nutrients to minimize the effect of resource depletion. Species were grown in the supernatant media, and their final density when grown of supernatant obtained from other species was compared to the density achieved when grown on their own supernatant by calculating a relative yield defined as: (density on other supernatant - density on self supernatant)/(density on other supernatant + density on self supernatant).

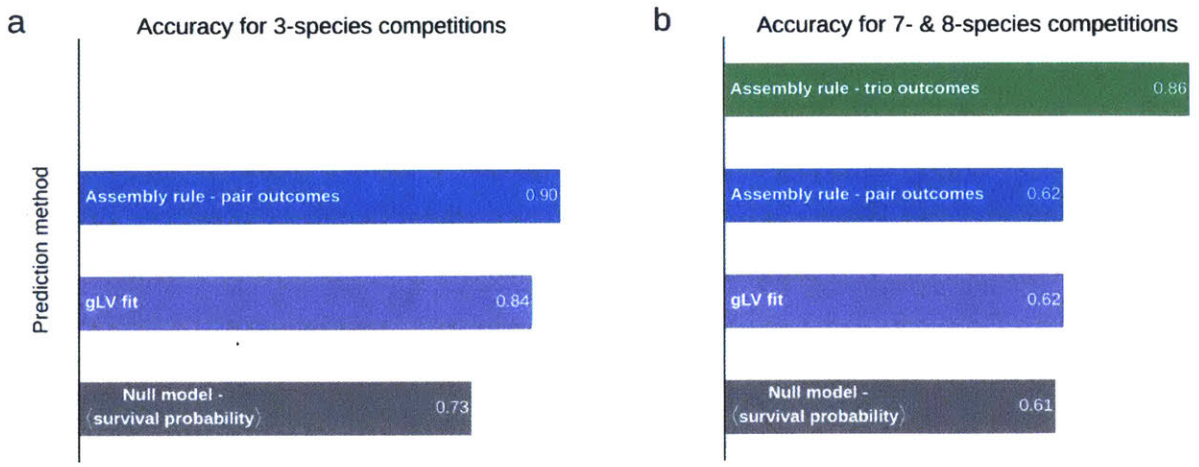

Supplementary Figure 3.6. The gLV model, fitted to experimental data, does not improve predictability over the assembly rule. gLV model parameters were inferred from time trajectories of monocultures and pairwise competitions (Supplementary Fig. 3.8). The inferred parameter values were used to simulate trio competitions (**a**) or competitions between sets of seven and eight species (**b**), and to predict species survival.

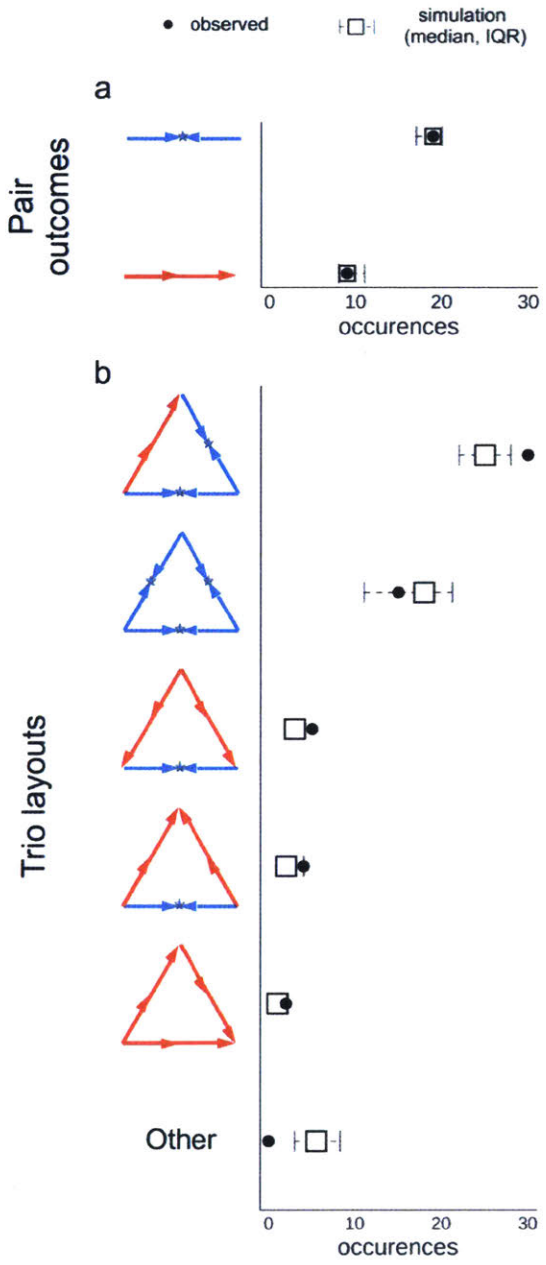

Supplementary Figure 3.7. gLV simulations recapitulate the experimentally observed proportions of pair outcomes, and yield a distribution of trio layouts similar to the observed one. a, gLV simulations included only pairs displaying competitive exclusion or coexistence, in proportions matching the experimentally observed ones. Bistable pairs that were generated in the simulation were discarded. **b**, The majority of trio layouts that occurred in the simulations were also observed experimentally, with a median of ~4/56 novel trio layouts occurring in the simulations. Medians and interquartile ranges (IQR) of occurrences in simulations are computed using 100 independent simulations. For each simulation, we created a set of eight species with random interactions strengths (α_{ij}) independently drawn from normal distribution with a mean of 0.6 and a standard deviation of 0.46. Pairwise outcomes and trio layouts were determined from the interaction strengths.

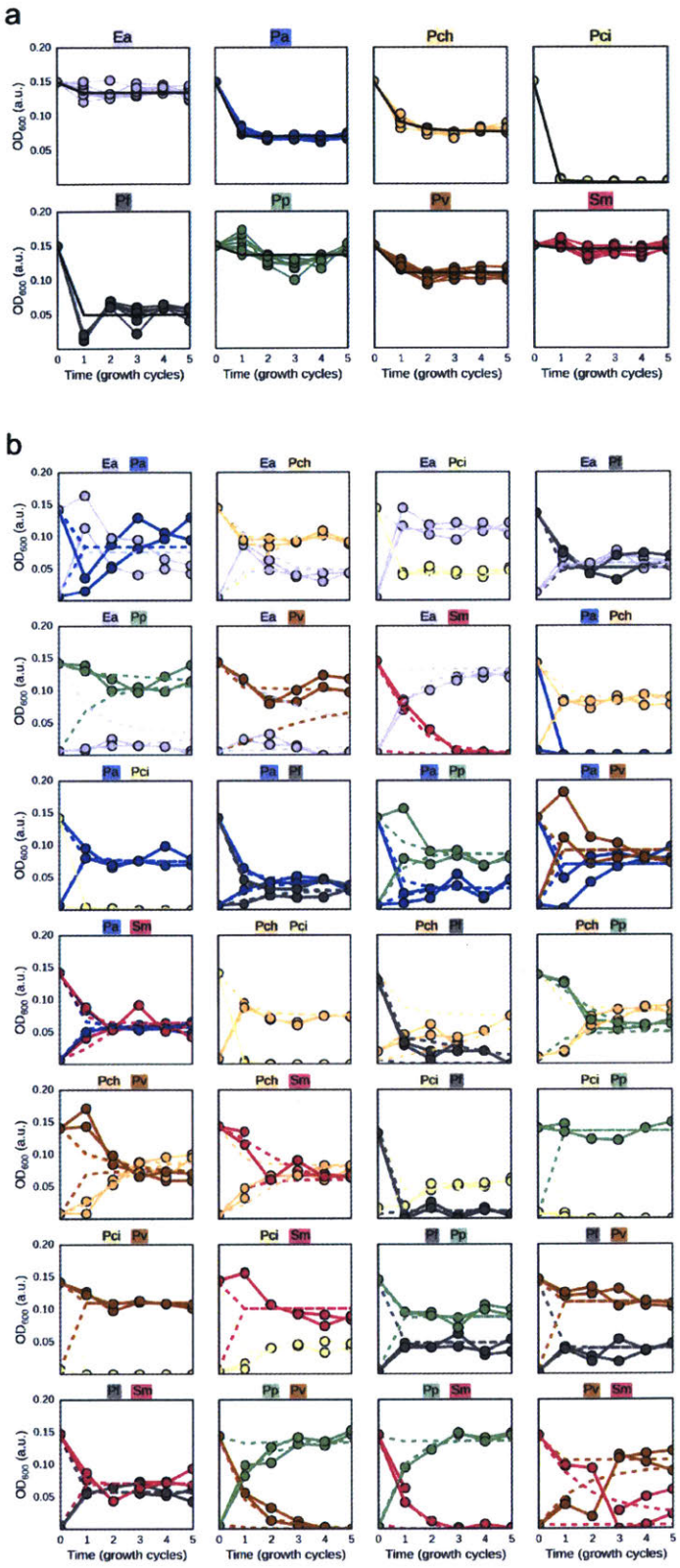

Supplementary Figure 3.8. gLV model parameters were fitted to the trajectories of monocultures and pair competitions. a, A growth rates (r) and carrying capacities (K) were

fitted to each monoculture trajectory, using eight replicates per species (Supplementary Table 3.2). **b**, Interaction coefficients (α_{ij}) were fitted to trajectories of pair competitions, using the inferred growth rates and carrying capacities (Supplementary Table 3.3). Each pair was competed in duplicate from two initial conditions where one species constituted 95% of the community and the other 5%. Some data are missing due to contamination or failed plating. Each species' OD was determined from the total culture OD and the species fractions, as measured by colony counting. Fits were done by simulating the growth and dilution cycles with gLV dynamics within a cycle, and minimizing the root-mean-square difference between the simulated dynamics and observed ones. The minimization was done using the Nelder-Mead method, as implemented in the *minimize* function from the python scipy package (v 0.16.0).

Supplementary Table 3.1. Trio competitions typically resulted in a stable community whose composition is independent of the starting fractions. Only a single trio (Pp, Pch, Sm) showed consistent bistability, with species survival depending on the initial community composition. Trios are sorted by layout and competitive outcomes. Species are ordered to match the layouts shown in Fig. 3.3. Survival (extinction) is indicated by a value of 1 (0). Survival values are not indicated for the two trios that did not display reproducible outcomes (Supplementary Fig. 3.4).

Competitors			Survival		
species A	species B	species C	species A	species B	species C
Ea	Pa	Sm	1	1	0
Ea	Pch	Pa	1	1	0
Ea	Pch	Sm	1	1	0
Ea	Pf	Sm	1	1	0
Pa	Ea	Pci	1	1	0
Pa	Pf	Pci	1	1	0
Pa	Sm	Pci	1	1	0
Pch	Ea	Pci	1	1	0
Pch	Ea	Pf	1	1	0
Pch	Pp	Pf	1	1	0
Pch	Sm	Pci	1	1	0
Pp	Ea	Pv	1	1	0
Pp	Pa	Pv	1	1	0
Pp	Pa	Sm	1	1	0
Pp	Pch	Pa	1	1	0
Pp	Pf	Pci	1	1	0
Pp	Pf	Pv	1	1	0
Pp	Pf	Sm	1	1	0
Pv	Pch	Pa	1	1	0
Pv	Pf	Pci	1	1	0
Pv	Sm	Pci	1	1	0
Sm	Pch	Pa	1	1	0
Ea	Pci	Sm	1	1	1
Pch	Pv	Pf	1	1	1
Pch	Sm	Pf	1	1	1
Pp	Ea	Pci	1	1	1
Pp	Pch	Pv	0	1	1
Pp	Pch	Sm	1 0	1 1	0 1
Ea	Pv	Sm	na	na	na
Pv	Ea	Pci	na	na	na
Pf	Pa	Sm	1	1	1
Pf	Pci	Ea	1	1	1
Pf	Pp	Ea	1	1	1
Pf	Pv	Ea	1	1	1

Competitors			Survival		
species A	species B	species C	species A	species B	species C
Pf	Sm	Pci	1	1	1
Pp	Pa	Ea	1	1	1
Pv	Pa	Ea	1	1	1
Pv	Pch	Ea	1	1	1
Pf	Pa	Ea	0	1	1
Pf	Pa	Pp	0	1	1
Pf	Pa	Pv	0	1	1
Pf	Sm	Pv	0	1	1
Pp	Pch	Ea	0	1	1
Sm	Pa	Pv	0	1	1
Sm	Pv	Pch	0	1	1
Pci	Pp	Pa	0	1	1
Pci	Pp	Pch	0	1	1
Pci	Pv	Pa	0	1	1
Pci	Pv	Pch	0	1	1
Sm	Pp	Ea	0	1	1
Pch	Pf	Pci	1	0	0
Pf	Pch	Pa	1	0	0
Pp	Sm	Pci	1	0	0
Pp	Sm	Pv	1	1	1
Pci	Pch	Pa	0	1	0
Pv	Pp	Pci	0	1	0

Supplementary Table 3.2. Inferred growth rates and carrying capacities. Growth rates and carrying capacities were found by fitting the time trajectories of each species to the gLV model (Supplementary Fig. 3.8). Note that in the case of single species, the gLV model simplifies to the logistic growth model. Given values were found by jointly fitting the data from all replicates. Errors indicate the standard-deviation of parameter values when fitted to each replicate separately.

	r	K
Ea	0.46 ± 0.02	0.13 ± 0.007
Pa	0.55 ± 0.07	0.07 ± 0.007
Pch	0.18 ± 0.07	0.11 ± 0.006
Pci	0.16 ± 0.03	0.01 ± 0.0005
Pf	0.25 ± 0.08	0.05 ± 0.007
Pp	0.65 ± 0.09	0.14 ± 0.009
Pv	0.57 ± 0.06	0.11 ± 0.005
Sm	0.34 ± 0.03	0.15 ± 0.006

Supplementary Table 3.3. Inferred interspecies interaction parameters. Note that these are interaction parameters (a_{ij}) which are not normalized by the carrying capacity. The corresponding gLV equations are:

$$\dot{N}_i = r_i N_i \left(1 - \frac{\sum_j a_{ij} N_j}{K_i}\right)$$

	Ea	**Pa**	**Pch**	**Pci**	**Pf**	**Pp**	**Pv**	**Sm**
Ea	1	0.69	1.09	0.55	1.53	0.82	1.09	0.72
Pa	-0.18	1	2.44	-2.58	1.13	0.43	0.01	0.21
Pch	-0.11	-0.8	1	-15.75	0.29	-0.04	-0.05	-0.03
Pci	-0.32	0	0.18	1	-3.39	0	0.05	-0.3
Pf	-0.02	0.28	1.2	0.83	1	0.01	0.07	-0.1
Pp	0.87	1.58	1.24	0.24	1	1	1.01	0.84
Pv	0.83	0.28	0.47	0	-0.02	0.79	1	0.7
Sm	0.96	1.23	1.42	1.21	1.31	0.91	0.98	1